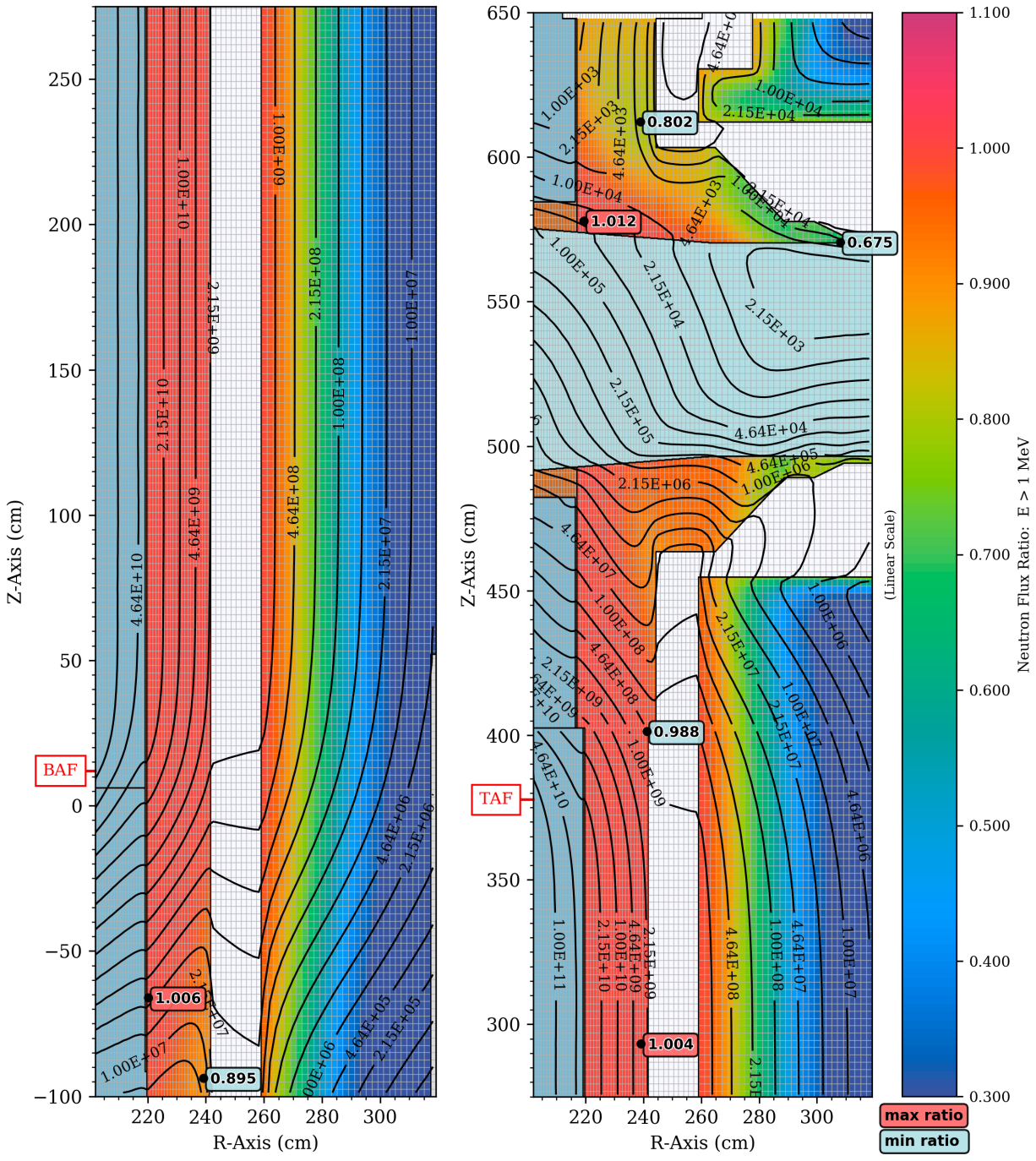

(a) Z = -100 to 275 cm

(b) Z = 275 to 650 cm

Figure 64. Fast neutron flux (E > 1 MeV) in the PWR reference model with NBS04 concrete in the bioshield, and the fast flux ratio when the bioshield concrete is modeled as **magnetite with steel punchings** concrete. The core is modeled as a spatially uniform ^{235}U fission source. The elevation view is at **292.5**°, the centerline of the outlet nozzle. The fast flux ratio in the RV, nozzles, and concrete is shown using flooded contours and contour lines. All other regions are colored based on their material assignments. The values inside the shaded boxes are the minimum and maximum ratios in the RV, nozzles, at this azimuthal angle. The minimum and maximum values in (b) are shown separately for the portions of the RV below and above 402.59 cm, where the thickness of the RV changes.

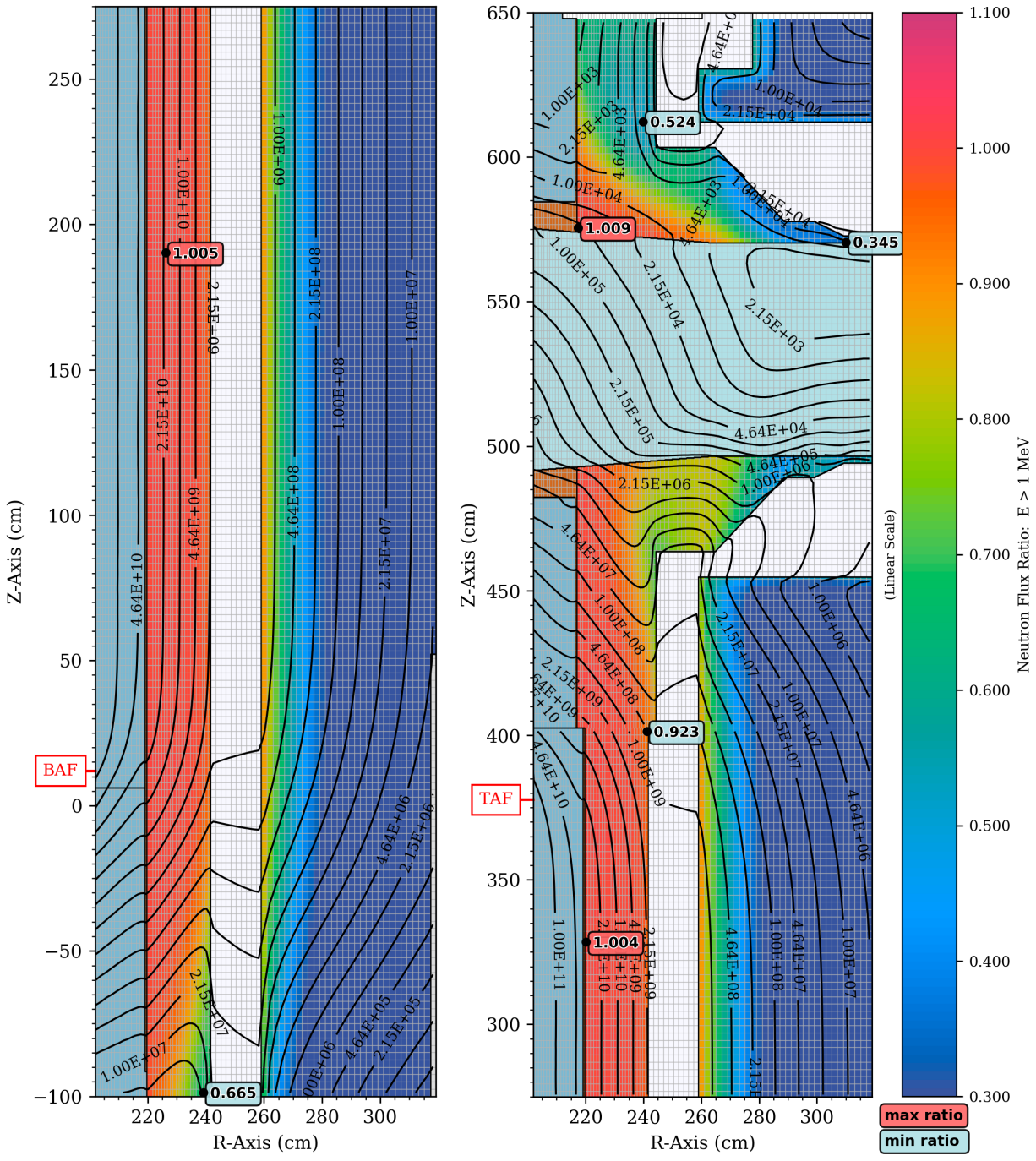

(a) Z = -100 to 275 cm

(b) Z = 275 to 650 cm

Figure 65. Fast neutron flux (E > 1 MeV) in the PWR reference model with NBS04 concrete in the bioshield, and the fast flux ratio when the bioshield concrete is modeled as **limonite with steel punchings** concrete. The core is modeled as a spatially uniform ^{235}U fission source. The elevation view is at **292.5**°, the centerline of the outlet nozzle. The fast flux ratio in the RV, nozzles, and concrete is shown using flooded contours and contour lines. All other regions are colored based on their material assignments. The values inside the shaded boxes are the minimum and maximum ratios in the RV, nozzles, at this azimuthal angle. The minimum and maximum values in (b) are shown separately for the portions of the RV below and above 402.59 cm, where the thickness of the RV changes.

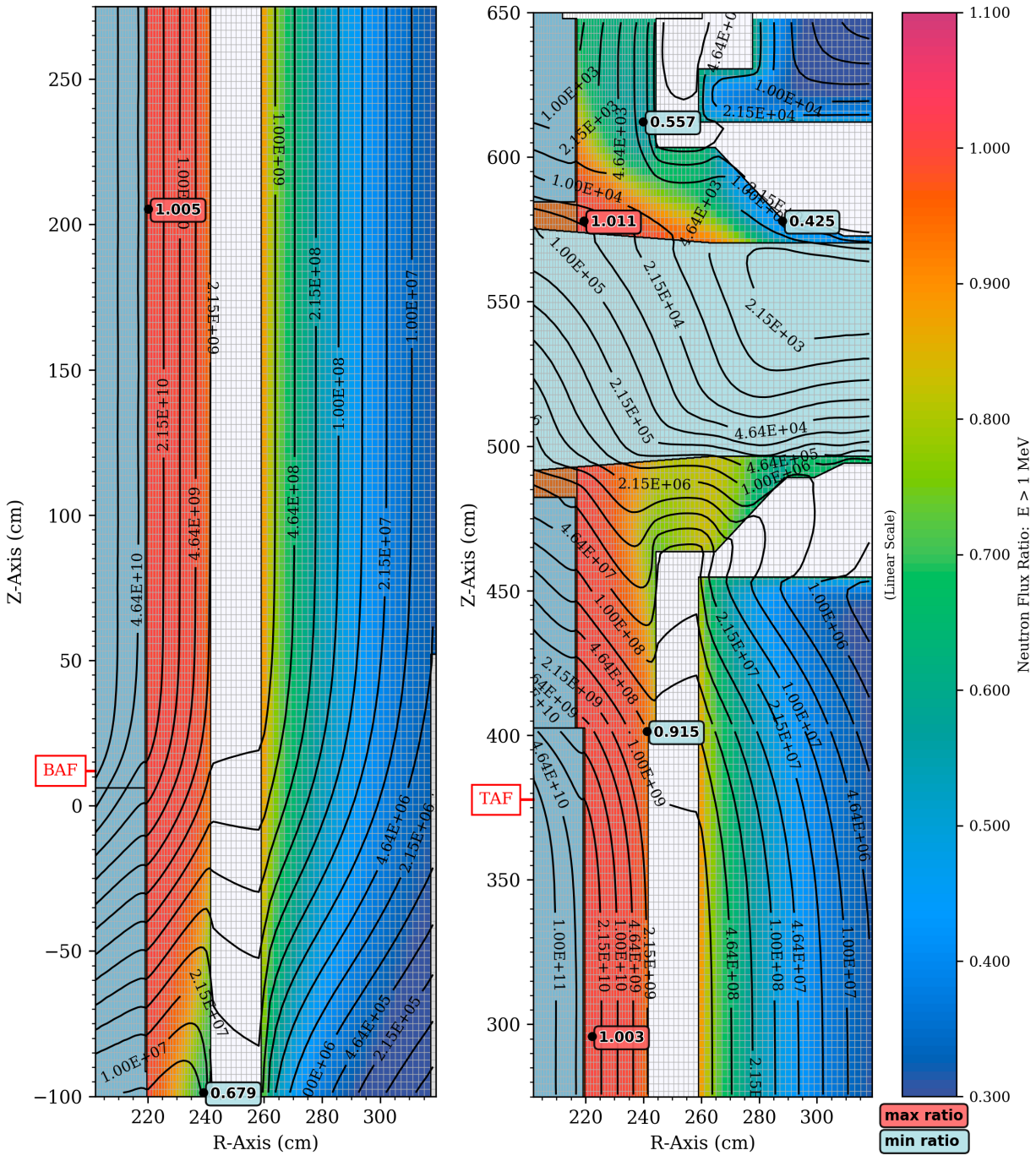

(a) Z = -100 to 275 cm

(b) Z = 275 to 650 cm

Figure 66. Fast neutron flux (E > 1 MeV) in the PWR reference model with NBS04 concrete in the bioshield, and the fast flux ratio when the bioshield concrete is modeled as **serpentine** concrete. The core is modeled as a spatially uniform ^{235}U fission source. The elevation view is at **292.5**°, the centerline of the outlet nozzle. The fast flux ratio in the RV, nozzles, and concrete is shown using flooded contours and contour lines. All other regions are colored based on their material assignments. The values inside the shaded boxes are the minimum and maximum ratios in the RV, nozzles, at this azimuthal angle. The minimum and maximum values in (b) are shown separately for the portions of the RV below and above 402.59 cm, where the thickness of the RV changes.

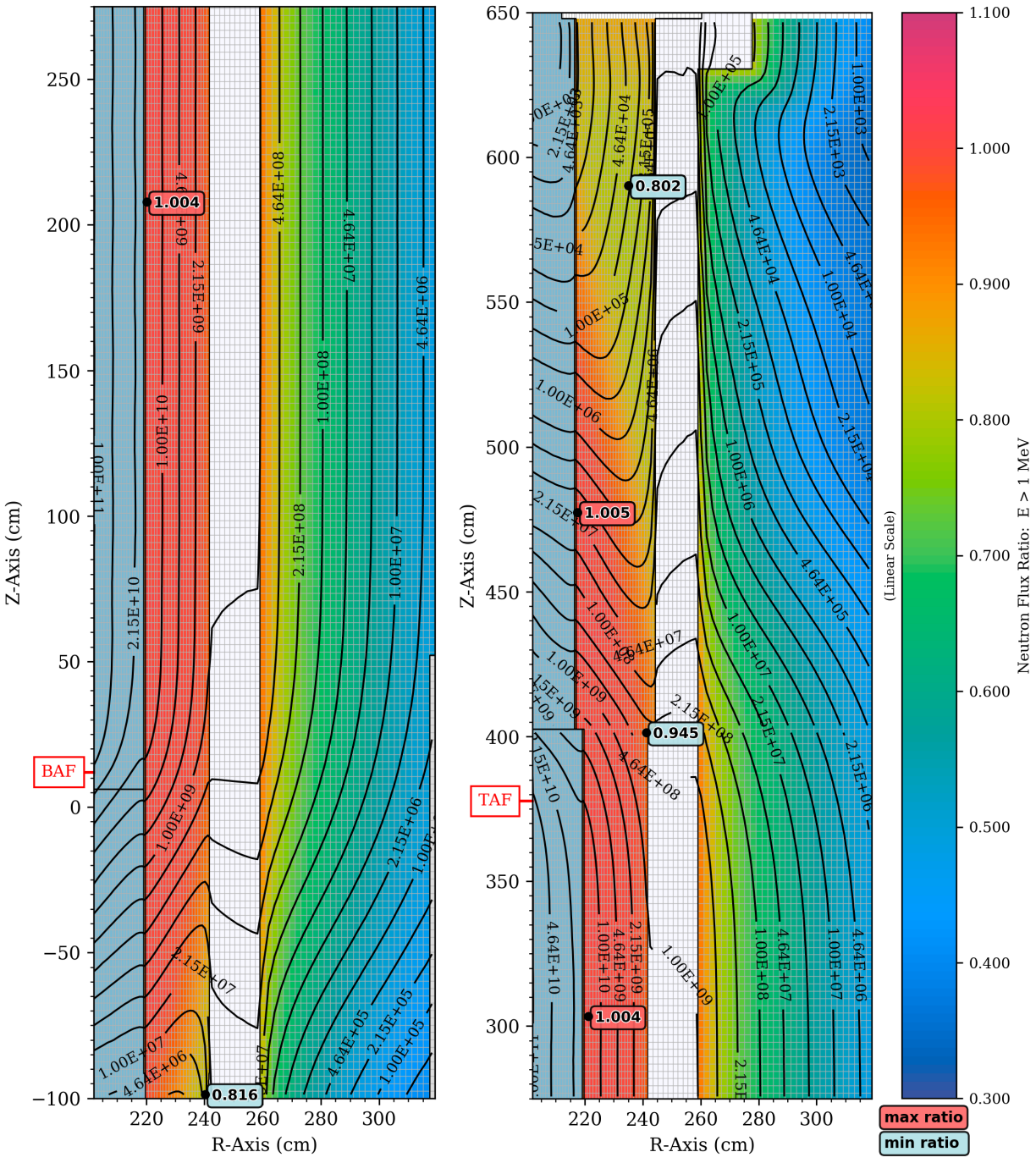

(a) Z = -100 to 275 cm

(b) Z = 275 to 650 cm

Figure 67. Fast neutron flux (E > 1 MeV) in the PWR reference model with NBS04 concrete in the bioshield, and the fast flux ratio when the bioshield concrete is modeled as **PNNL reduced H** concrete. The core is modeled as a spatially uniform ^{235}U fission source. The elevation view is at **270.5**°, which has the maximum amount of water between the core and the RV. The fast flux ratio in the RV and concrete is shown using flooded contours and contour lines. All other regions are colored based on their material assignments. The values inside the shaded boxes are the minimum and maximum ratios in the RV at this azimuthal angle. The minimum and maximum values in (b) are shown separately for the portions of the RV below and above 402.59 cm, where the thickness of the RV changes.

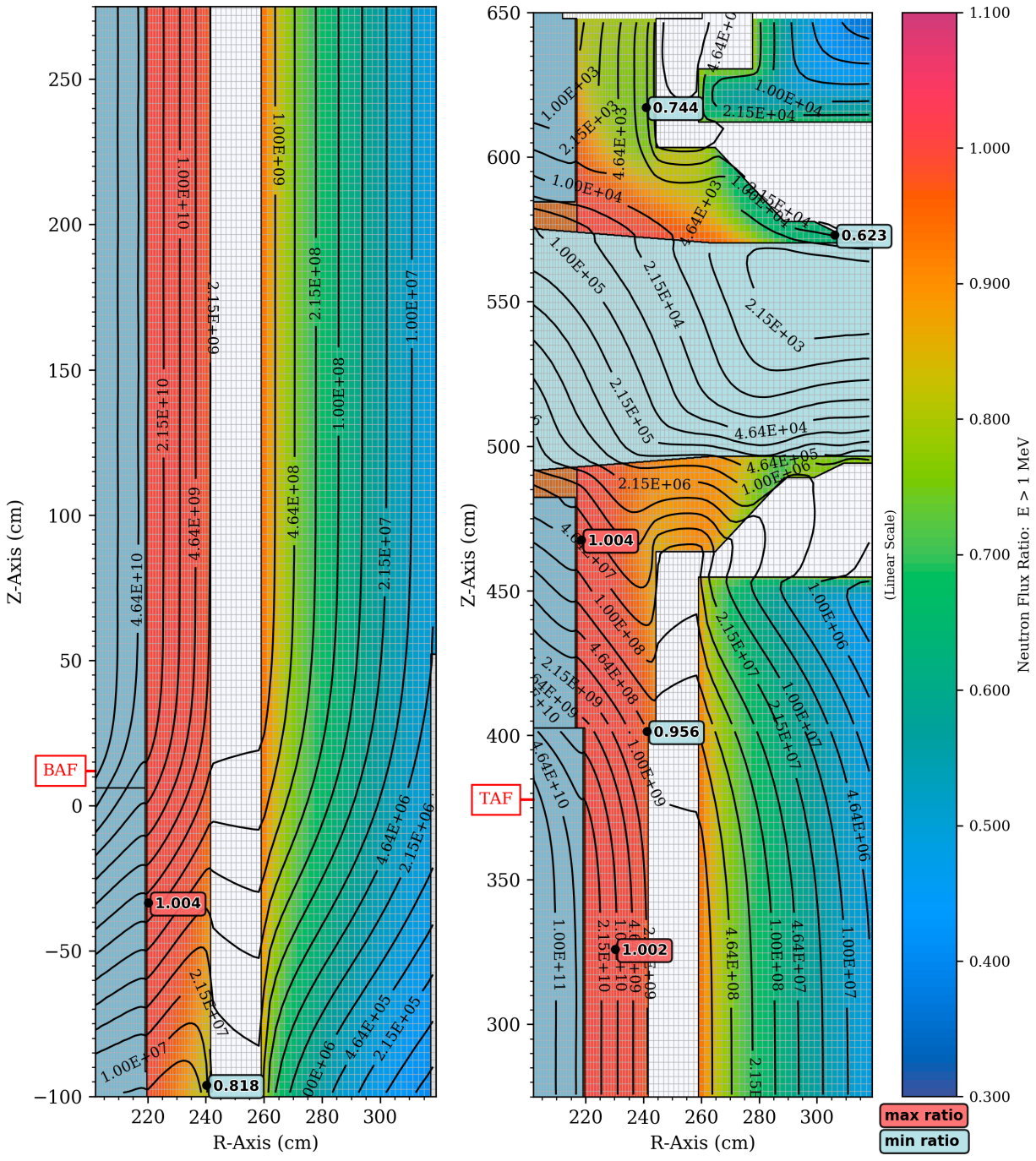

(a) Z = -100 to 275 cm

(b) Z = 275 to 650 cm

Figure 68. Fast neutron flux (E > 1 MeV) in the PWR reference model with NBS04 concrete in the bioshield, and the fast flux ratio when the bioshield concrete is modeled as **PNNL reduced H** concrete. The core is modeled as a spatially uniform ^{235}U fission source. The elevation view is at **292.5**°, the centerline of the outlet nozzle. The fast flux ratio in the RV, nozzles, and concrete is shown using flooded contours and contour lines. All other regions are colored based on their material assignments. The values inside the shaded boxes are the minimum and maximum ratios in the RV, nozzles, at this azimuthal angle. The minimum and maximum values in (b) are shown separately for the portions of the RV below and above 402.59 cm, where the thickness of the RV changes.

6 Reactor Cavity Gap Parameter Study

For reactor vessel locations above and below the beltline region, the effect of neutrons that scatter in the bioshield and stream up the gap between the RV and the bioshield becomes progressively more important at increasing distances. At sufficient distances from the core, these gap streaming neutrons can reverse the direction of the flux gradient in the RV, with the maximum flux occurring on the outer surface and the minimum flux on the inner surface (see Figures 34 and 35). This behavior has been noted in previous studies, including "Comparison of Regulatory Guide 1.99 Fluence Attenuation Methods" [30].

Figures 21–27 and Figures 29–35 in Section 3 illustrate the effect of cavity streaming, showing the fast flux in the RV for a spatially spatially uniform ^{235}U source. This cavity streaming effect suggests that the geometry of the RV/bioshield gap, and the composition of the bioshield concrete, may have a significant effect on RV flux levels outside the beltline region. The effect of changes in the concrete composition was addressed in Section 5.

To assess the impact of the reactor cavity gap width on the gap streaming effect, changes in the gap width were made in the reference PWR model. The baseline model, shown in Figure 69a, has a gap width of 17.38 cm below 402.59 cm (where the vessel thickness increases slightly) and 14.76 cm from 402.59 cm to 647.86 cm (where the vessel flange begins). The perturbed models have gap width increases of 10, 20, and 30 cm. Figure 69b shows the model with the gap width increased by 30 cm.

For each of these revised models, the fluxes were calculated using the baseline representation of the core, with a spatially uniform ^{235}U fission source. In addition, the fluxes for each model were calculated using a spatially uniform ^{239}Pu fission source. The concrete bioshield was modeled using NBS04 concrete and also with PNNL ordinary concrete, which has the maximum hydrogen content of the concrete compositions evaluated in Section 5, for the ^{235}U source.

Figures 70–72 show the flux ratios on the inner and outer surfaces of the RV for the increased gap widths of 10, 20, and 30 cm with the spatially uniform ^{235}U source. Because of the large range in the flux ratios (up to nearly a factor of 20 above the nozzles in the +30 cm model) the ratios are plotted using logarithmic scaling. Two-dimensional RZ plots of the flux ratios at two azimuthal locations (270.5° and 292.5°) are shown in Figures 74–79.

Figures 70–72 show that the effect of cavity streaming becomes more pronounced as the gap size is increased for this model. The wider annular gap not only opens up a larger streaming path between the RV and the bioshield, but it also changes the scattering angles for neutrons scattered from the bioshield back into the cavity gap.

As a result of the increased cavity streaming, the fast neutron flux at the outer surface of the RV increases substantially (by factors of ~4–9) outside the traditional beltline region at azimuthal angles away from the nozzles (see Figures 74, 76, and 78). For regions that include a nozzle in the cavity gap, the increase in the fast flux is even more significant in the nozzle structure and in the RV above the nozzles.

It can also be seen that within the height of the active fuel, there is a slight decrease in the fast flux at the outer radius of the RV, which becomes more pronounced as the gap width increases. However, this effect is inconsequential, as the fast flux at the outer surface of the RV is nearly an order of magnitude lower than the fast flux at the inner RV surface.

While this is not an exhaustive study of cavity gap widths, the results of this study confirm that changes in

the reactor cavity geometry have a much more pronounced effect on fluence outside the traditional beltline region than within that region.

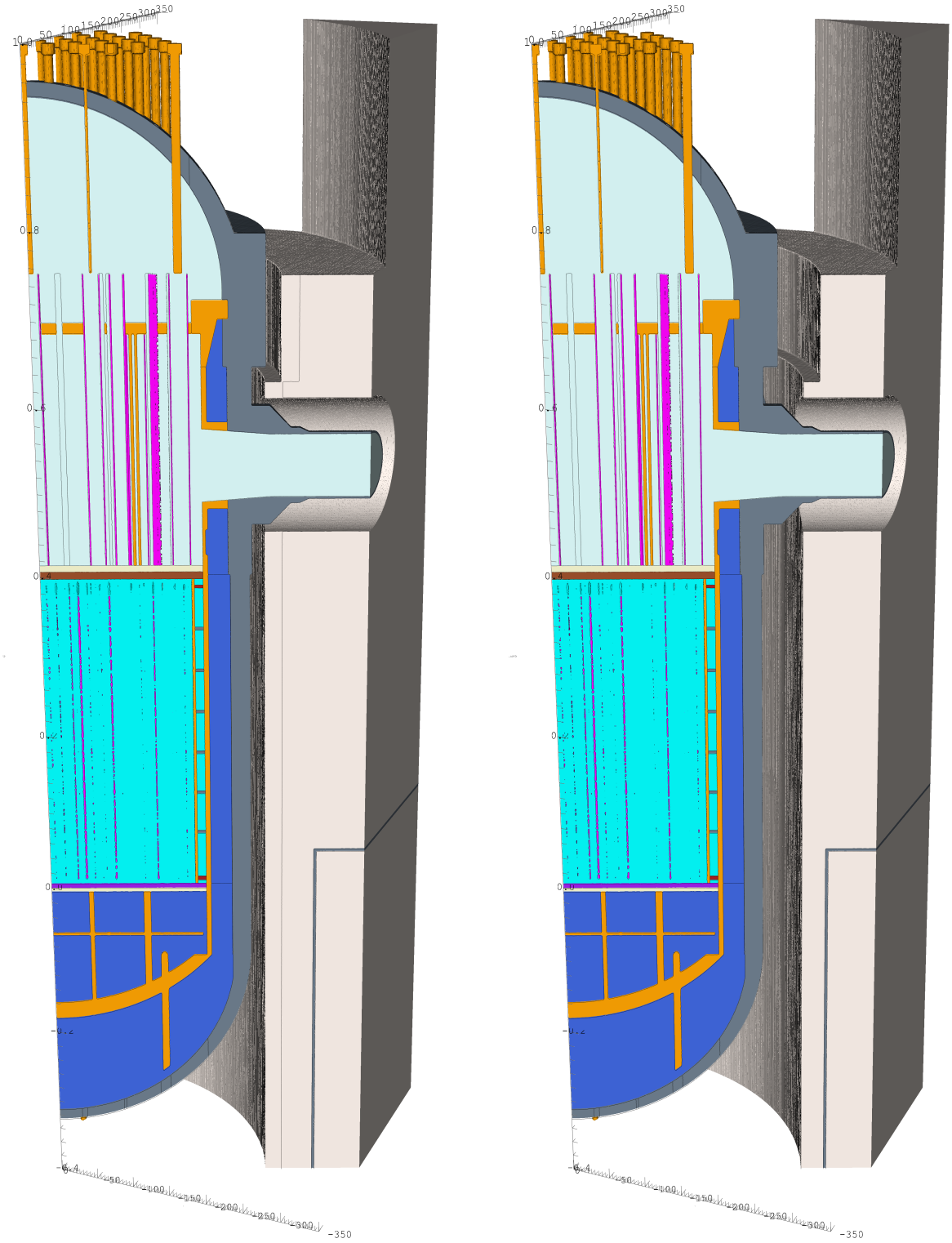

(a) Baseline model

(b) Model with increased cavity gap width

Figure 69. View of the PWR reference model with a cut plane through the center of the outlet nozzle: (a) baseline model with cavity gap widths of 17.38 cm below 402.59 cm (where the RV thickness increases slightly) and 14.76 cm from 402.59 to 746.86 cm (where the flange begins); (b) model with the cavity gap widths increased by 30 cm relative to the baseline model.

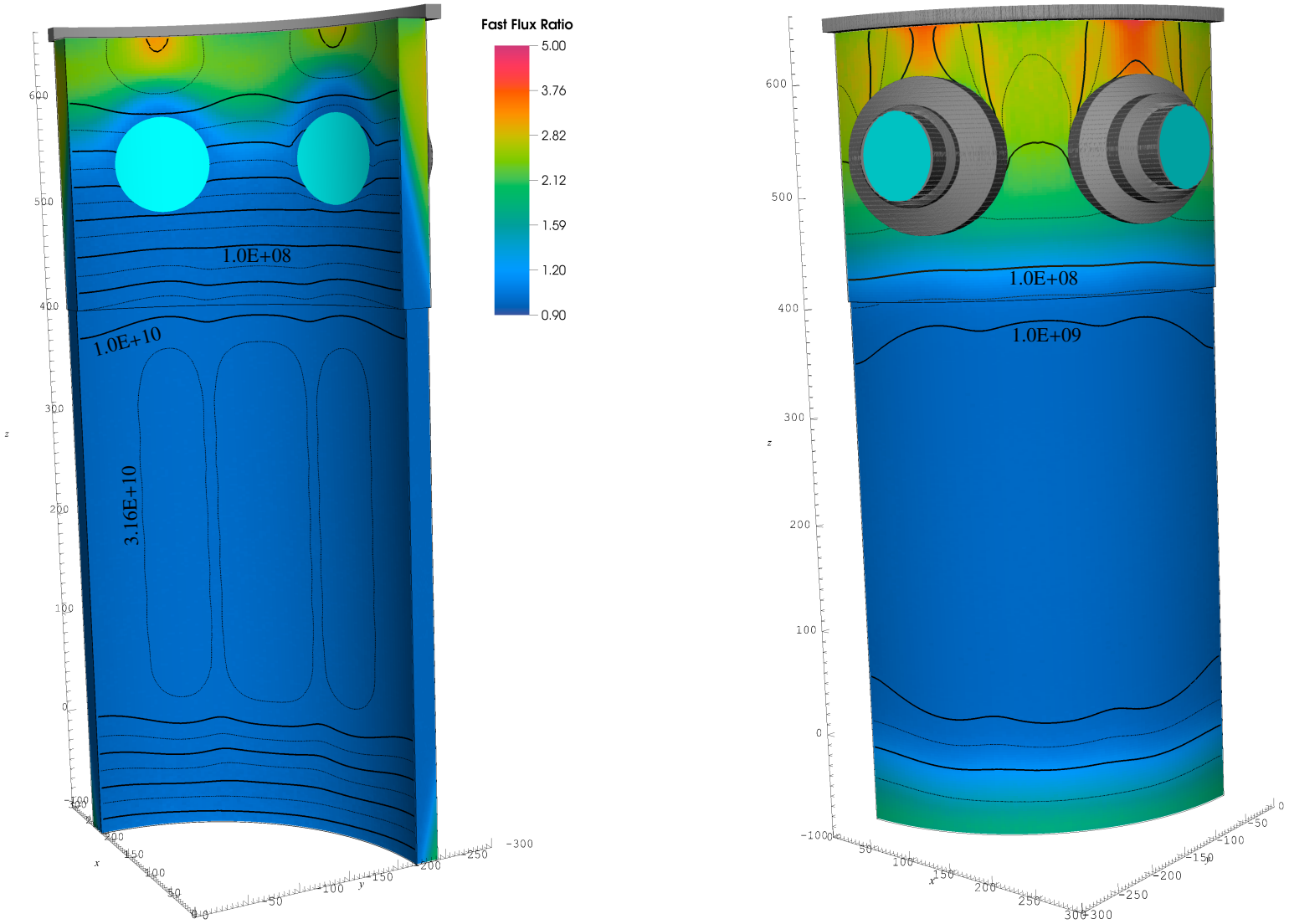

Figure 70. Ratio of the fast neutron flux (E > 1 MeV) on the inner and outer surfaces of the PWR reference model RV when the cavity gap width is **increased by 10 cm**. The core is modeled as a spatially uniform ^{235}U fission source. The cyan regions represent the coolant in the inlet and outlet nozzles. The contour lines correspond to the fast flux for the baseline model. The reduction in flux between each pair of solid contour lines is one decade. The thinner dashed lines are a factor of 3.16 below/above the adjacent solid contours.

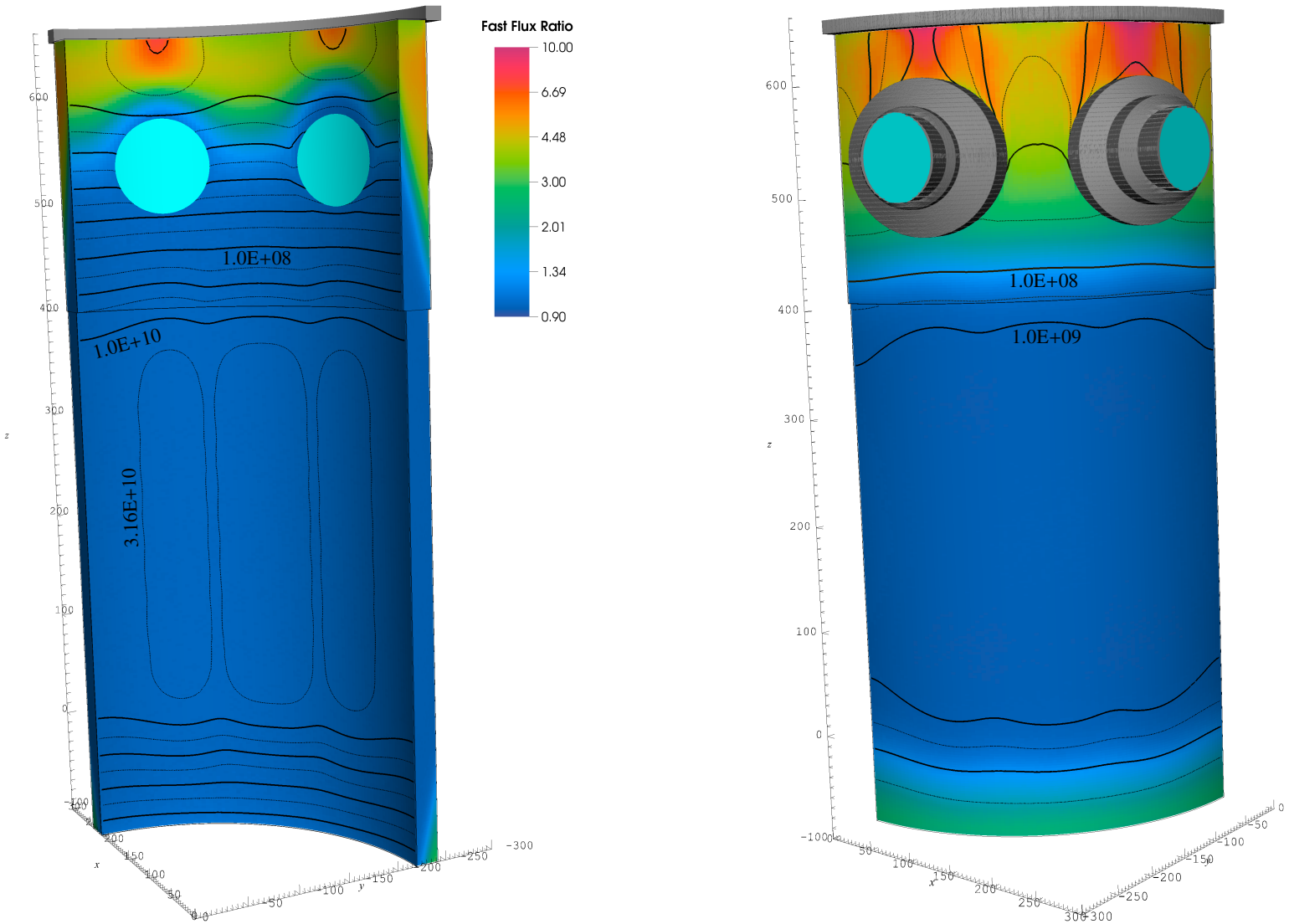

Figure 71. Ratio of the fast neutron flux (E > 1 MeV) on the inner and outer surfaces of the PWR reference model RV when the cavity gap width is **increased by 20 cm**. The core is modeled as a spatially uniform ^{235}U fission source. The cyan regions represent the coolant in the inlet and outlet nozzles. The contour lines correspond to the fast flux for the baseline model. The reduction in flux between each pair of solid contour lines is one decade. The thinner dashed lines are a factor of 3.16 below/above the adjacent solid contours.

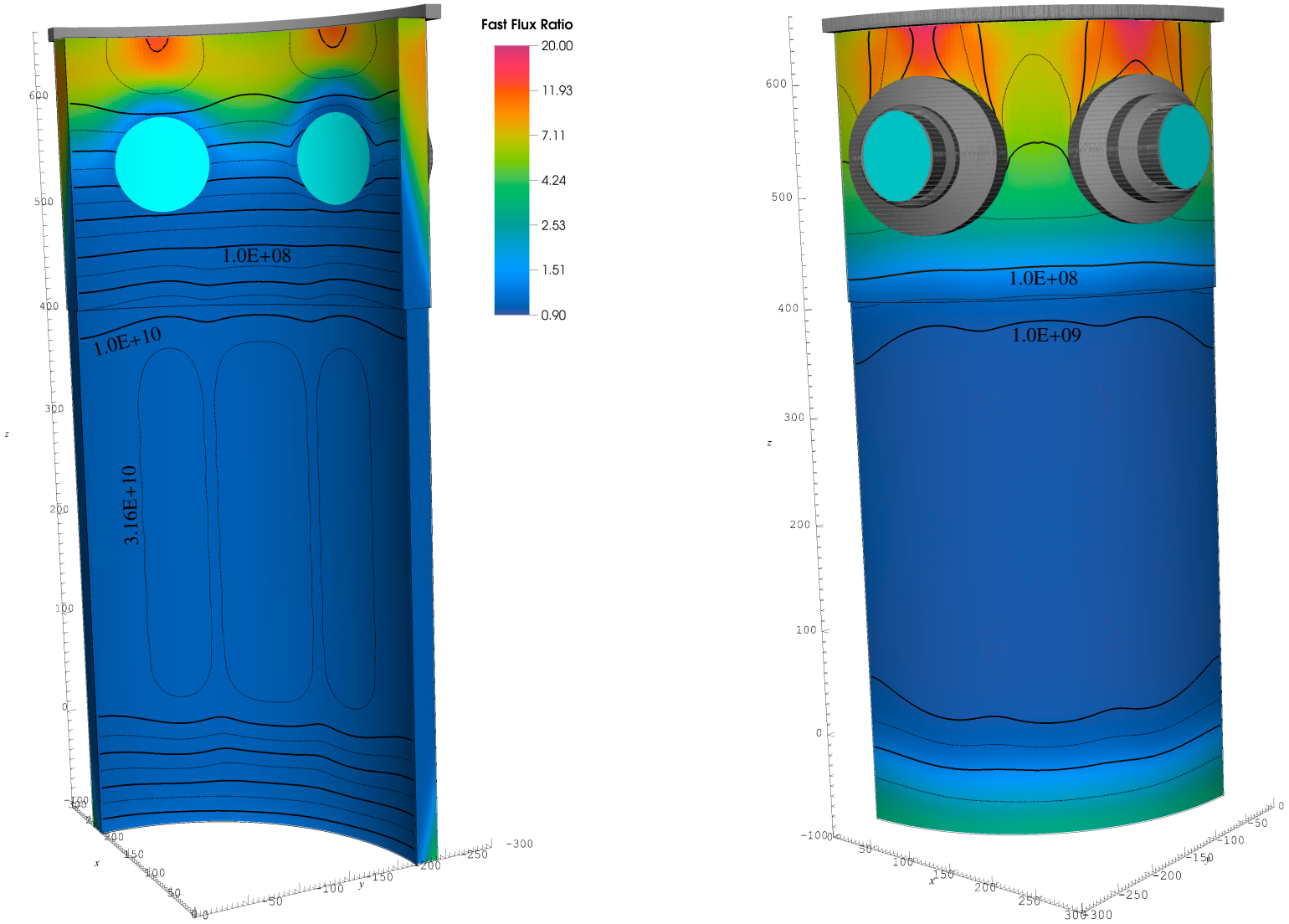

Figure 72. Ratio of the fast neutron flux (E > 1 MeV) on the inner and outer surfaces of the PWR reference model RV when the cavity gap width is **increased by 30 cm**. The core is modeled as a spatially uniform ^{235}U fission source. The cyan regions represent the coolant in the inlet and outlet nozzles. The contour lines correspond to the fast flux for the baseline model. The reduction in flux between each pair of solid contour lines is one decade. The thinner dashed lines are a factor of 3.16 below/above the adjacent solid contours.

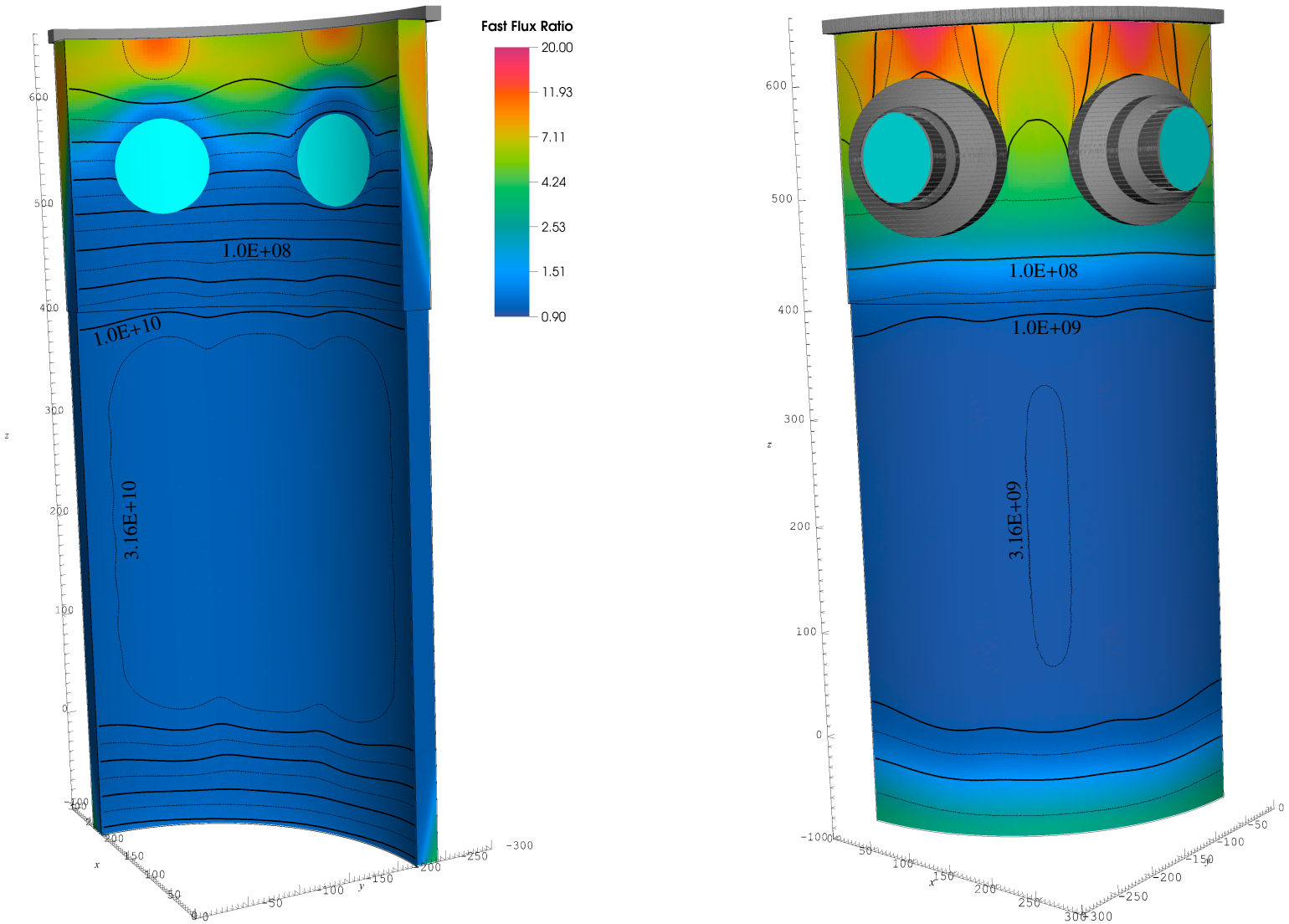

Figure 73. Ratio of the fast neutron flux (E > 1 MeV) on the inner and outer surfaces of the PWR reference model RV when the cavity gap width is **increased by 30 cm**. The core is modeled as a spatially uniform ^{239}Pu fission source. The cyan regions represent the coolant in the inlet and outlet nozzles. The contour lines correspond to the fast flux for the baseline model. The reduction in flux between each pair of solid contour lines is one decade. The thinner dashed lines are a factor of 3.16 below/above the adjacent solid contours.

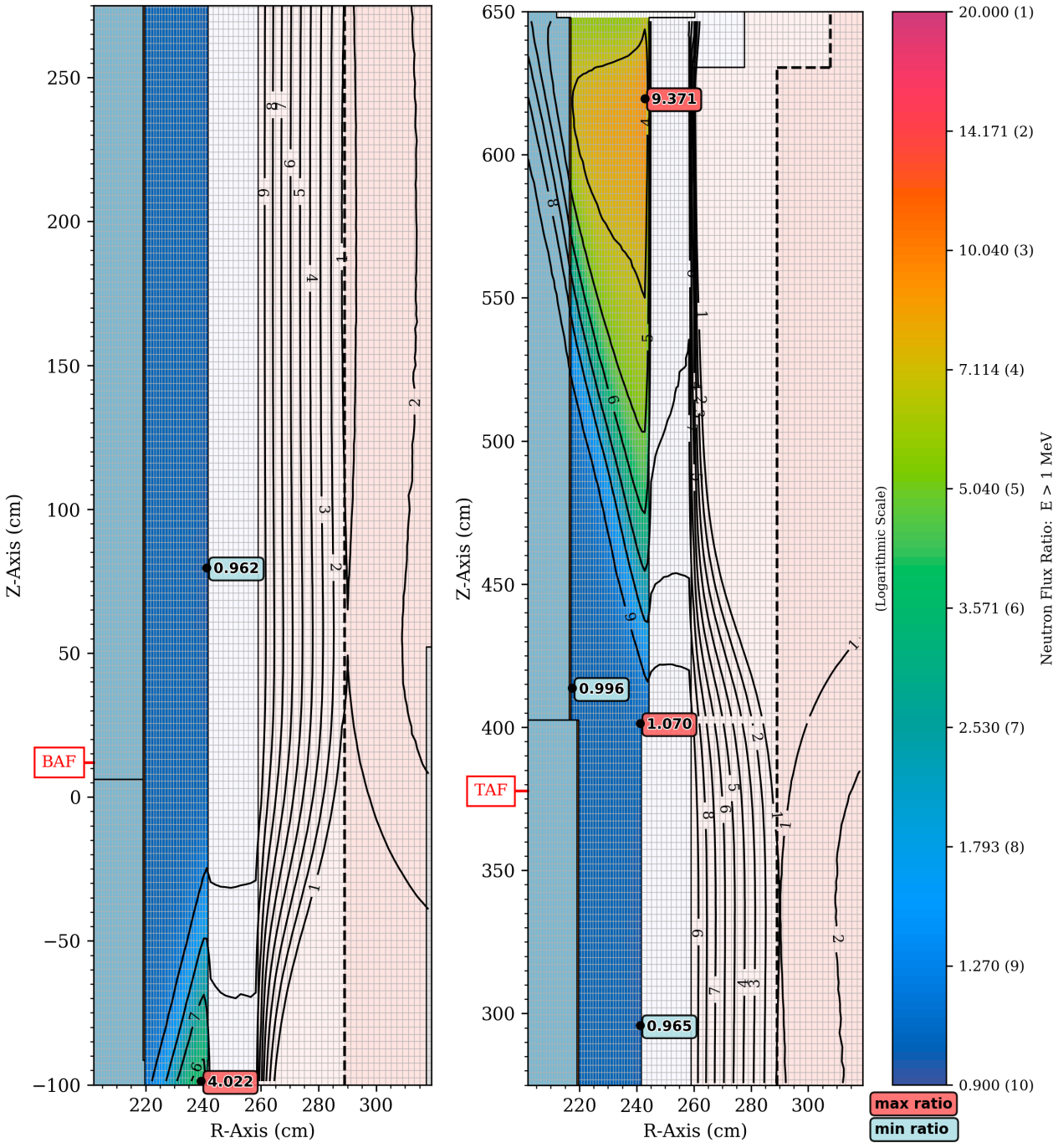

(a) Z = -100 to 275 cm

(b) Z = 275 to 650 cm

Figure 74. Fast neutron flux (E > 1 MeV) in the PWR reference model with the baseline cavity gap width, and the fast flux ratio when the cavity gap widths are **increased by 30 cm**. The source is modeled as a spatially uniform ^{235}U fission source. The bioshield is **NBS04** concrete. The elevation view is at **270.5**°, which has the maximum amount of water between the core and the RV. The fast flux ratio in the RV is shown using flooded contours and contour lines. All other regions are colored based on their material assignments. The dashed vertical lines indicate the inner radius of the bioshield for the gap width increase of 30 cm. The lightly shaded inner portion of the bioshield represents the concrete that is lost for the 30-cm gap increase. The values inside the shaded boxes are the minimum and maximum ratios in the RV at this azimuthal angle. The minimum and maximum values in (b) are shown separately for the portions of the RV below and above 402.59 cm, where the thickness of the RV changes.

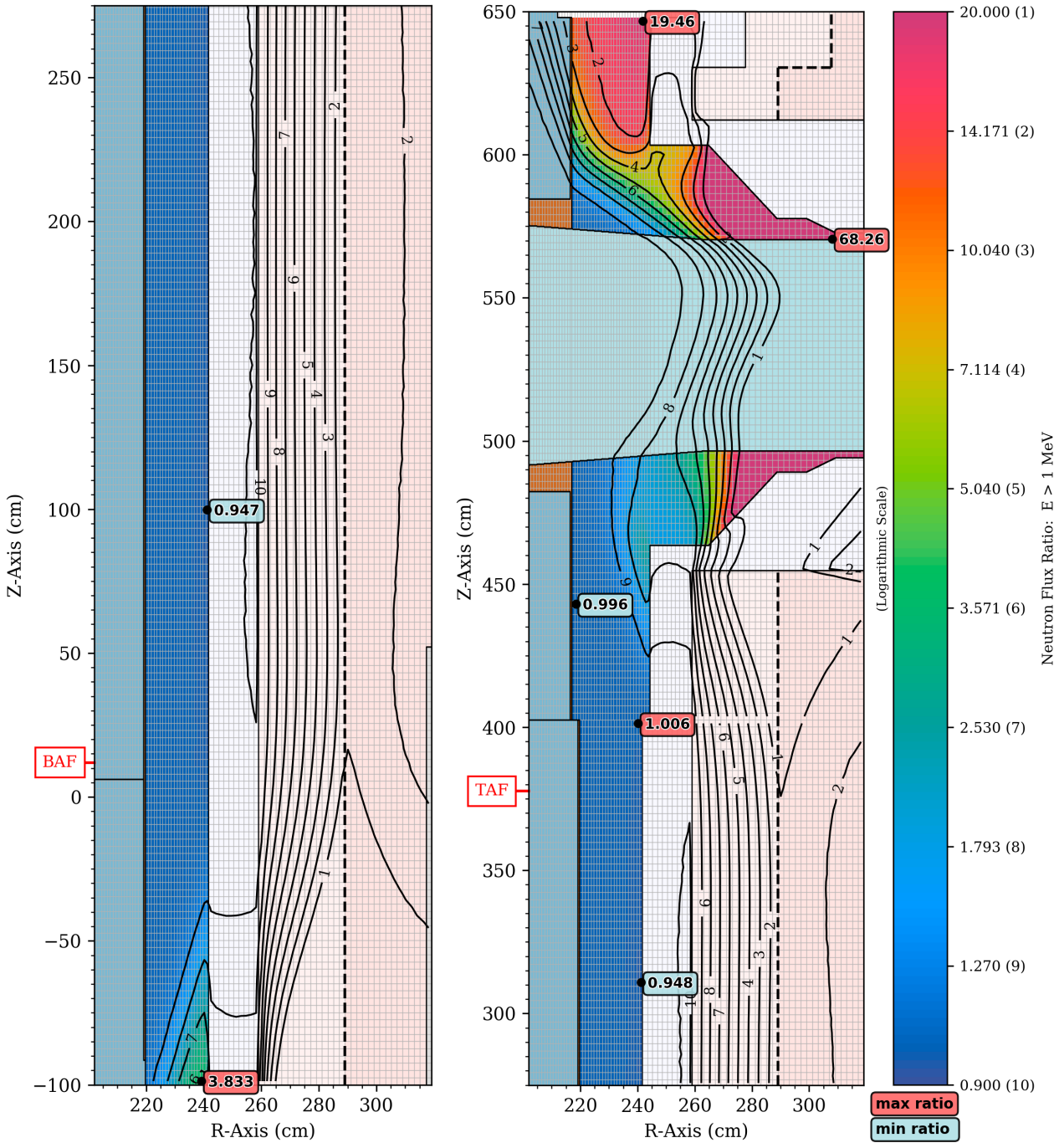

(a) Z = -100 to 275 cm

(b) Z = 275 to 650 cm

Figure 75. Fast neutron flux (E > 1 MeV) in the PWR reference model with the baseline cavity gap width, and the fast flux ratio when the cavity gap widths are **increased by 30 cm**. The source is modeled as a spatially uniform ^{235}U fission source. The bioshield is **NBS04** concrete. The elevation view is at **292.5**°, which is the centerline of the outlet nozzle. The fast flux ratio in the RV and the nozzles is shown using flooded contours and contour lines. All other regions are colored based on their material assignments. The dashed vertical lines indicate the inner radius of the bioshield for the gap width increase of 30 cm. The lightly shaded inner portion of the bioshield represents the concrete that is lost for the 30-cm gap increase. The values inside the shaded boxes are the minimum and maximum ratios in the RV and the nozzles at this azimuthal angle. The minimum and maximum values in (b) are shown separately for the portions of the RV below and above 402.59 cm, where the thickness of the RV changes.

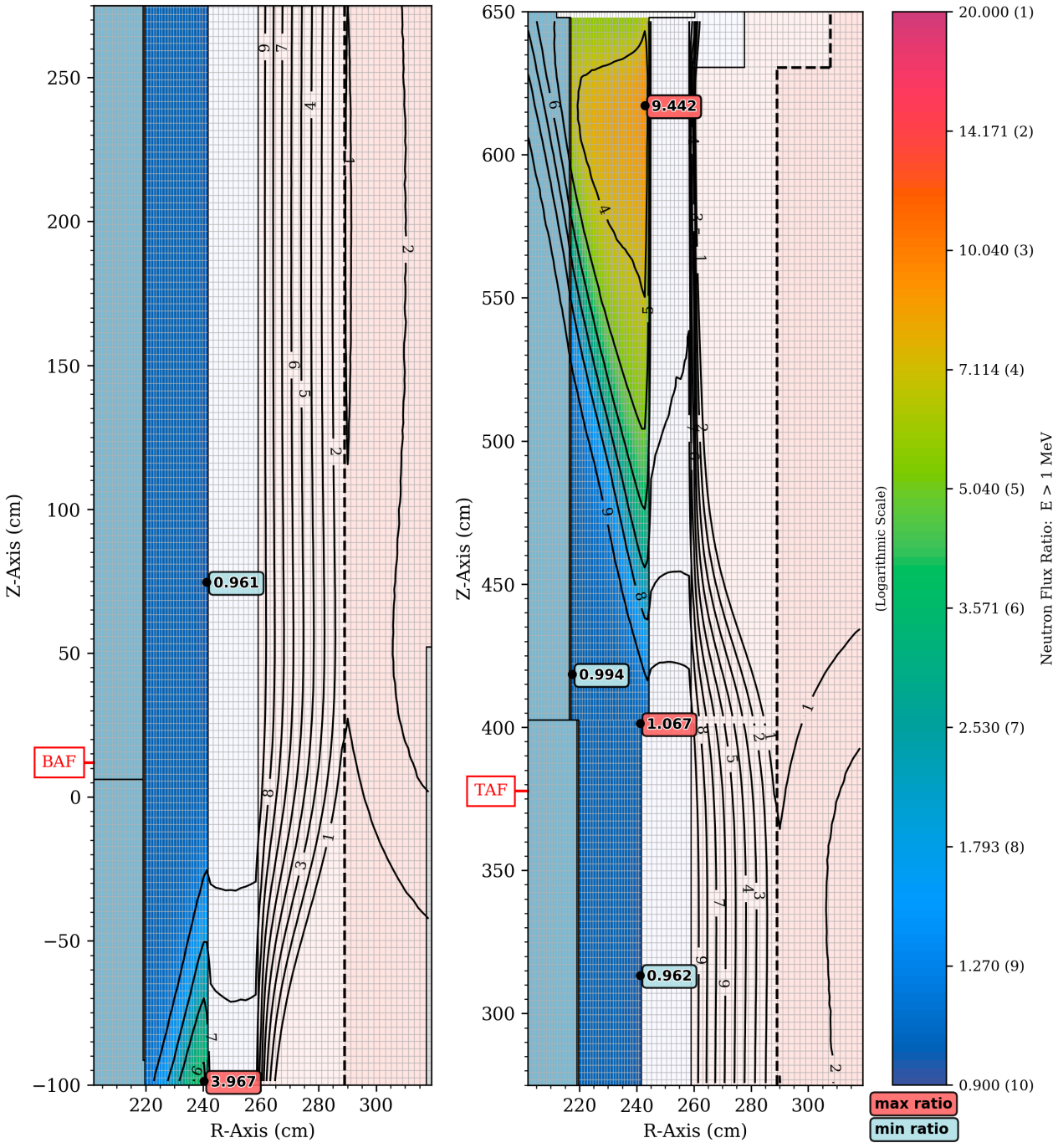

(a) Z = -100 to 275 cm

(b) Z = 275 to 650 cm

Figure 76. Fast neutron flux (E > 1 MeV) in the PWR reference model with the baseline cavity gap width, and the fast flux ratio when the cavity gap widths are **increased by 30 cm**. The source is modeled as a spatially uniform ^{239}Pu fission source. The bioshield is **NBS04** concrete. The elevation view is at **270.5**°, which has the maximum amount of water between the core and the RV. The fast flux ratio in the RV is shown using flooded contours and contour lines. All other regions are colored based on their material assignments. The dashed vertical lines indicate the inner radius of the bioshield for the gap width increase of 30 cm. The lightly shaded inner portion of the bioshield represents the concrete that is lost for the 30-cm gap increase. The values inside the shaded boxes are the minimum and maximum ratios in the RV at this azimuthal angle. The minimum and maximum values in (b) are shown separately for the portions of the RV below and above 402.59 cm, where the thickness of the RV changes.

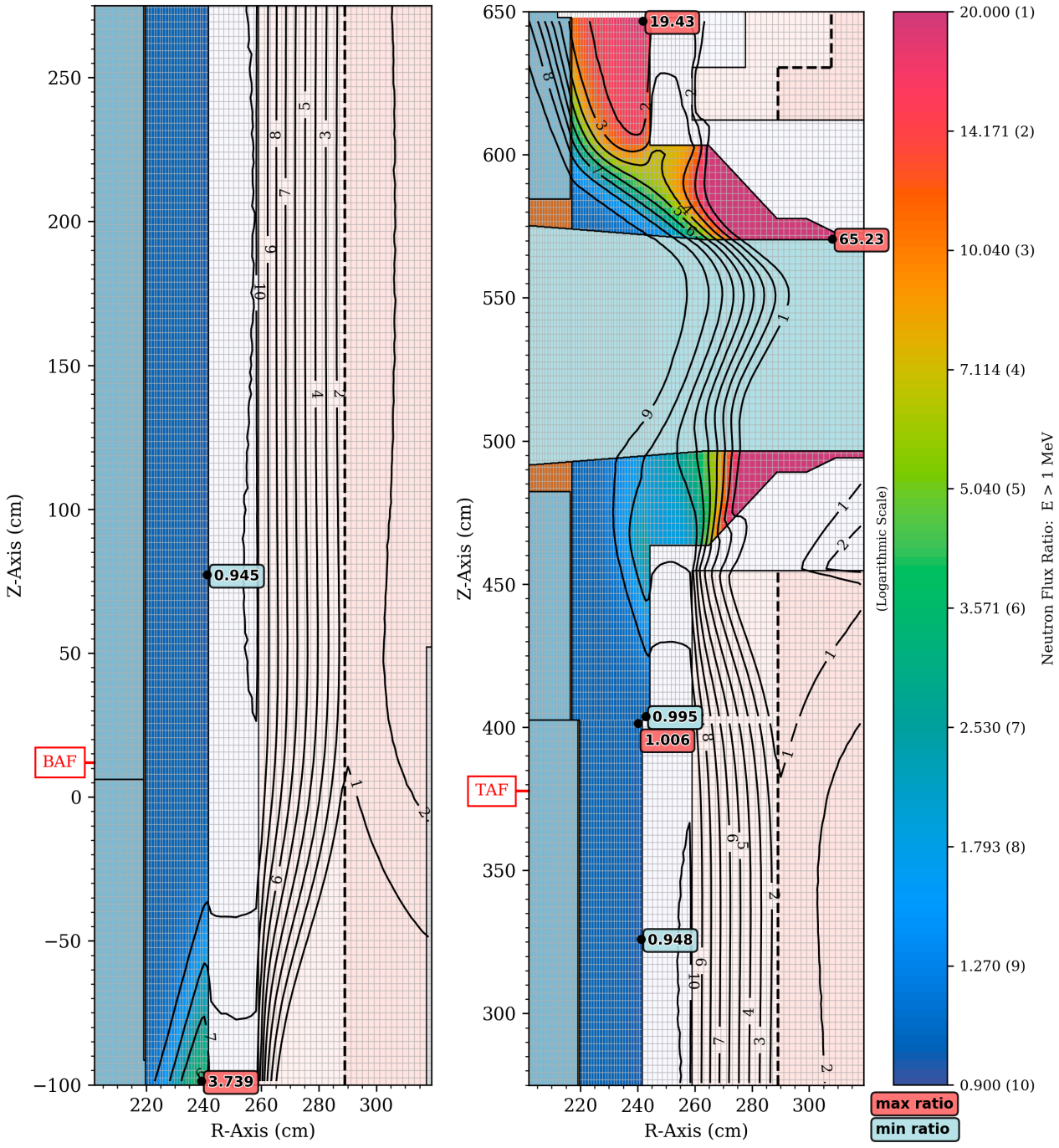

(a) Z = -100 to 275 cm

(b) Z = 275 to 650 cm

Figure 77. Fast neutron flux (E > 1 MeV) in the PWR reference model with the baseline cavity gap width, and the fast flux ratio when the cavity gap widths are **increased by 30 cm**. The source is modeled as a spatially uniform ^{239}Pu fission source. The bioshield is **NBS04** concrete. The elevation view is at **292.5**°, which is the centerline of the outlet nozzle. The fast flux ratio in the RV and the nozzles is shown using flooded contours and contour lines. All other regions are colored based on their material assignments. The dashed vertical lines indicate the inner radius of the bioshield for the gap width increase of 30 cm. The lightly shaded inner portion of the bioshield represents the concrete that is lost for the 30-cm gap increase. The values inside the shaded boxes are the minimum and maximum ratios in the RV and the nozzles at this azimuthal angle. The minimum and maximum values in (b) are shown separately for the portions of the RV below and above 402.59 cm, where the thickness of the RV changes.

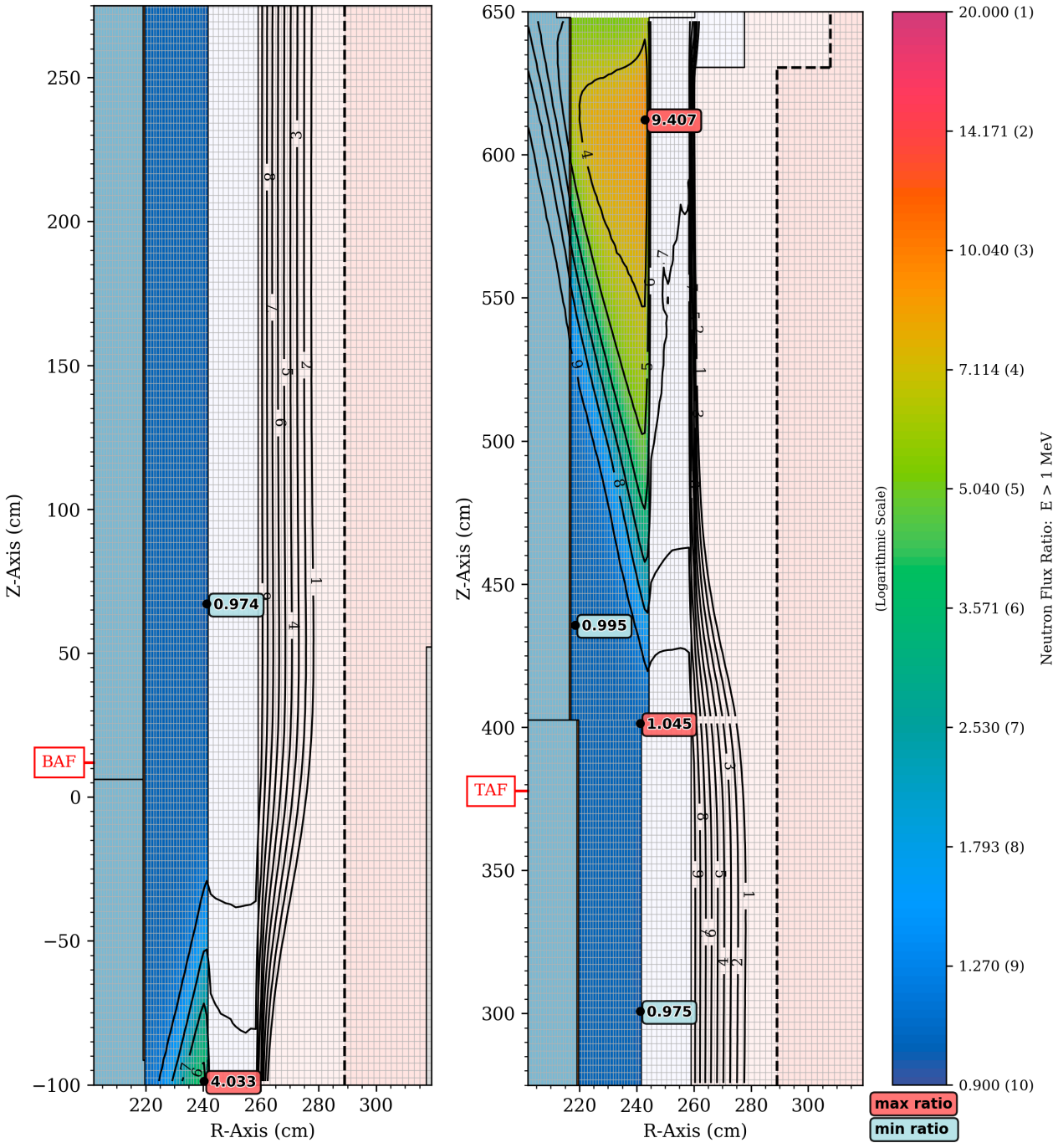

(a) Z = -100 to 275 cm

(b) Z = 275 to 650 cm

Figure 78. Fast neutron flux (E > 1 MeV) in the PWR reference model with the baseline cavity gap width, and the fast flux ratio when the cavity gap widths are **increased by 30 cm**. The source is modeled as a spatially uniform ^{235}U fission source. The bioshield is **PNNL ordinary** concrete. The elevation view is at **270.5**°, which has the maximum amount of water between the core and the RV. The fast flux ratio in the RV is shown using flooded contours and contour lines. All other regions are colored based on their material assignments. The dashed vertical lines indicate the inner radius of the bioshield for the gap width increase of 30 cm. The lightly shaded inner portion of the bioshield represents the concrete that is lost for the 30-cm gap increase. The values inside the shaded boxes are the minimum and maximum ratios in the RV at this azimuthal angle. The minimum and maximum values in (b) are shown separately for the portions of the RV below and above 402.59 cm, where the thickness of the RV changes.

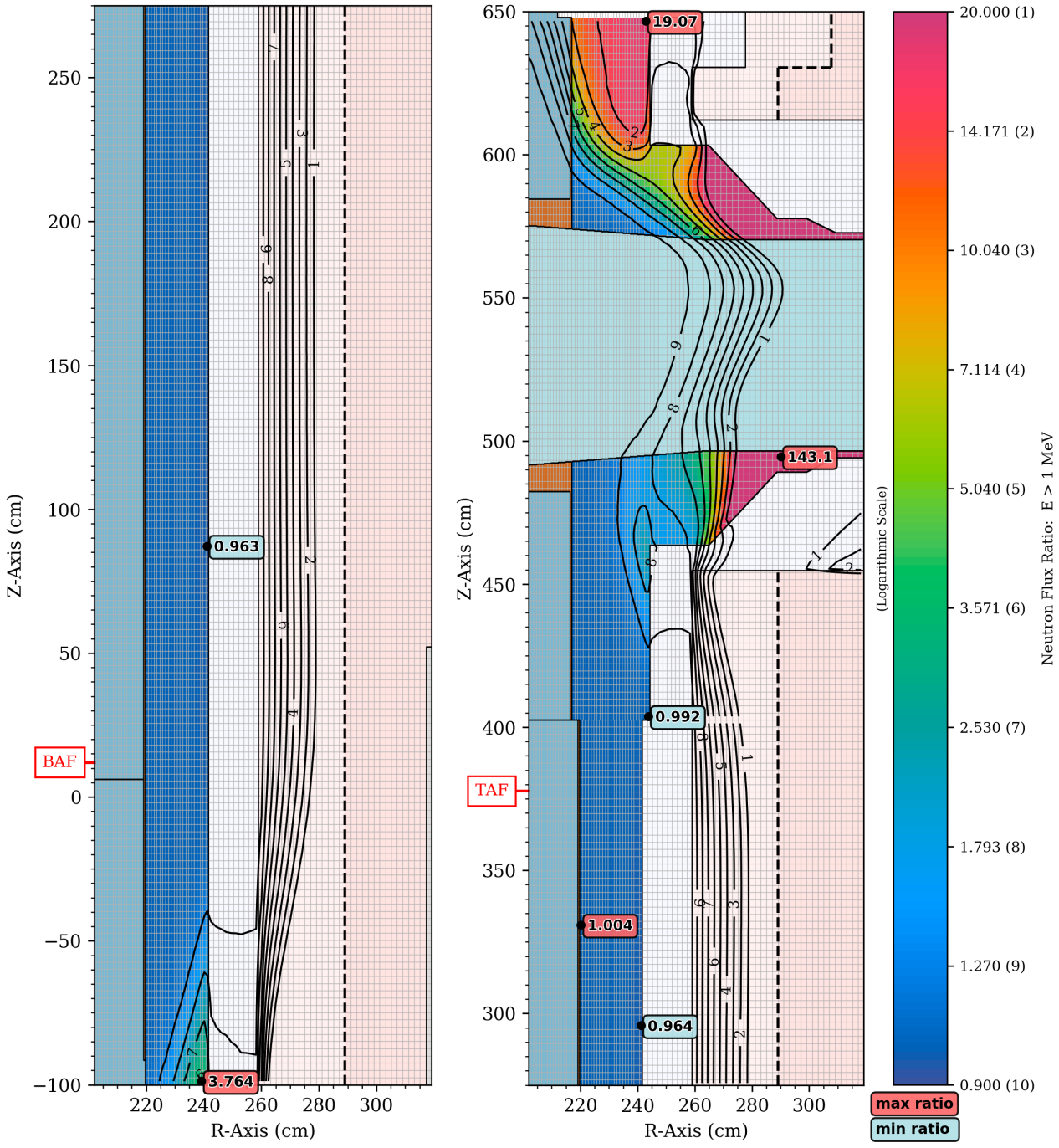

(a) Z = -100 to 275 cm

(b) Z = 275 to 650 cm

Figure 79. Fast neutron flux (E > 1 MeV) in the PWR reference model with the baseline cavity gap width, and the fast flux ratio when the cavity gap widths are **increased by 30 cm**. The source is modeled as a spatially uniform ^{235}U fission source. The bioshield is **PNNL ordinary** concrete. The elevation view is at **292.5**°, which is the centerline of the outlet nozzle. The fast flux ratio in the RV and the nozzles is shown using flooded contours and contour lines. All other regions are colored based on their material assignments. The dashed vertical lines indicate the inner radius of the bioshield for the gap width increase of 30 cm. The lightly shaded inner portion of the bioshield represents the concrete that is lost for the 30-cm gap increase. The values inside the shaded boxes are the minimum and maximum ratios in the RV and the nozzles at this azimuthal angle. The minimum and maximum values in (b) are shown separately for the portions of the RV below and above 402.59 cm, where the thickness of the RV changes.

7 Water Temperature Parameter Study

Changes in the coolant temperature at any location within the reactor vessel and in the nozzles will affect neutron attenuation due to changes in the density of the coolant and hence the macroscopic cross section. While changes to the coolant temperature will also have an effect on resonance cross sections, that effect is very minor for the range of temperature changes considered in this study. For regions outside the traditional beltline, the effect of water temperature changes is likely to be more significant than it is in the beltline region, as the energy spectrum of cavity streaming neutrons will be different, and the scattering of neutrons in the inlet and outlet nozzles will also be affected.

To assess this effect, parametric changes were made to the water temperatures in the PWR model. The temperatures in all locations were changed by -15, -10, -5, +5, +10, and +15 °F. Note that these temperature changes are not intended to represent actual operating conditions, but rather to provide an assessment of how the fast flux in the RV—particularly outside the traditional beltline region—might change as a result of water temperature changes.

Figures 80–82 show the effect of reducing the water temperatures by 5, 10, and 15 °F. As the temperature is decreased, the density of the water increases, and there is more attenuation of the fission neutrons from the core to the RV. Note that the effect is most pronounced in the vicinity of the nozzles due to the significant amount of water within the nozzles. Figures 83–84 illustrate the fast flux ratio at two azimuthal locations when the water temperatures are reduced by 15 °F.

Figures 85–87 show the effect of increasing the water temperatures by 5, 10, and 15 °F. As the coolant temperature is increased, the density of the water decreases, and there is less attenuation of the fission neutrons as they are transported from the core to the RV. The effect is again most pronounced in the vicinity of the nozzles. Figures 88–89 illustrate the fast flux ratio at two azimuthal locations when the water temperatures are increased by 15 °F.

The results of the parametric water temperature study clearly indicate that the impact of changes in coolant temperature with respect to RV fluence levels is more significant for locations outside the traditional beltline region. This sensitivity indicates that accurate modeling of coolant temperatures throughout the RV and the nozzles as a function of the plant operating history (including power uprates of other changes that may affect coolant pressure and temperature) is important for extended beltline fluence calculations.

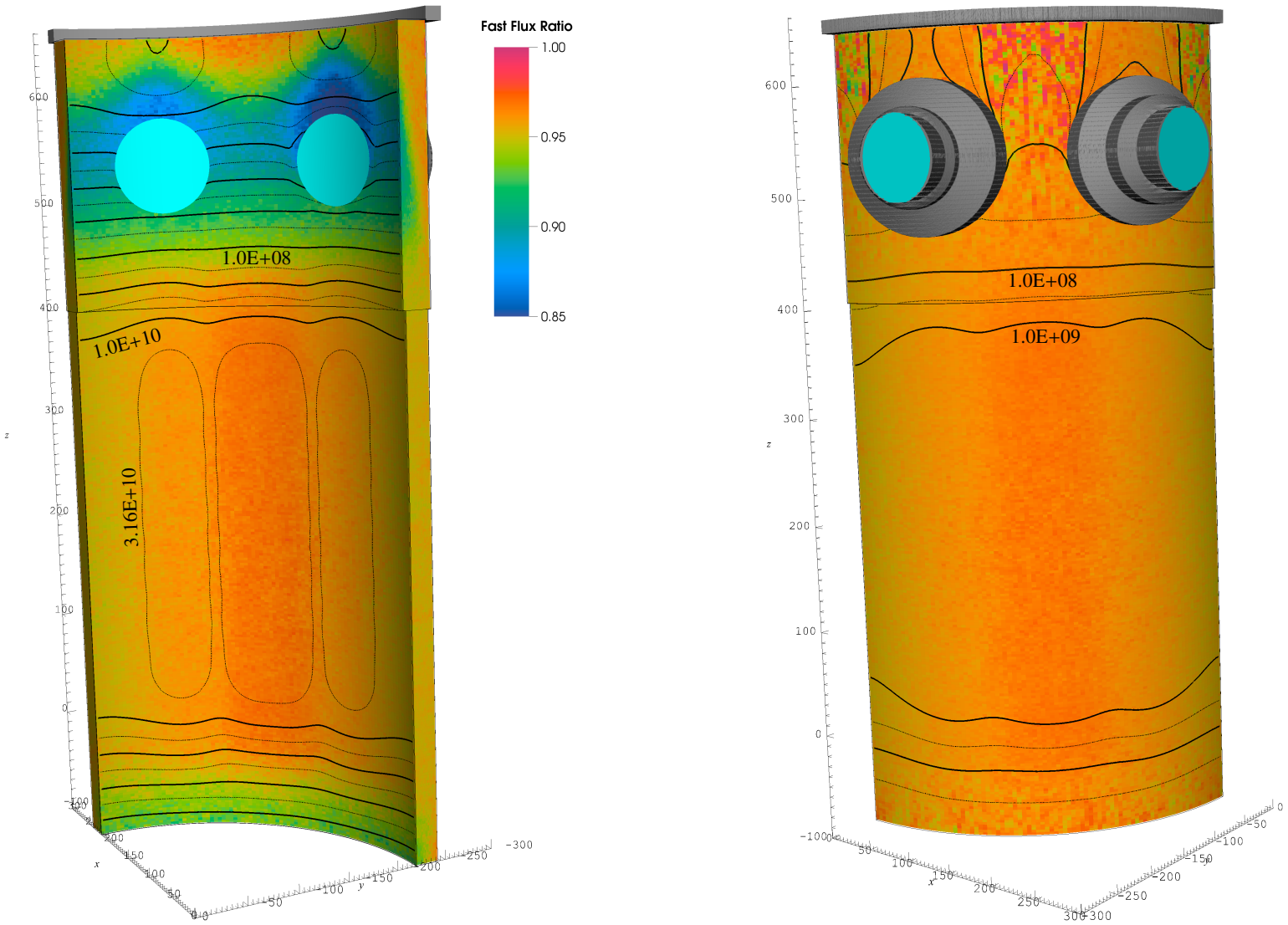

Figure 80. Ratio of the fast neutron flux (E > 1 MeV) on the inner and outer surfaces of the PWR reference model RV when water temperatures in all regions are **decreased by 5 °F**. The core is modeled as a spatially uniform ^{235}U fission source. The cyan regions represent the coolant in the inlet and outlet nozzles. Contour lines correspond to the fast flux for the baseline model. The reduction in flux between each pair of solid contour lines is one decade. Thinner dashed lines are a factor of 3.16 below/above the adjacent solid contours.

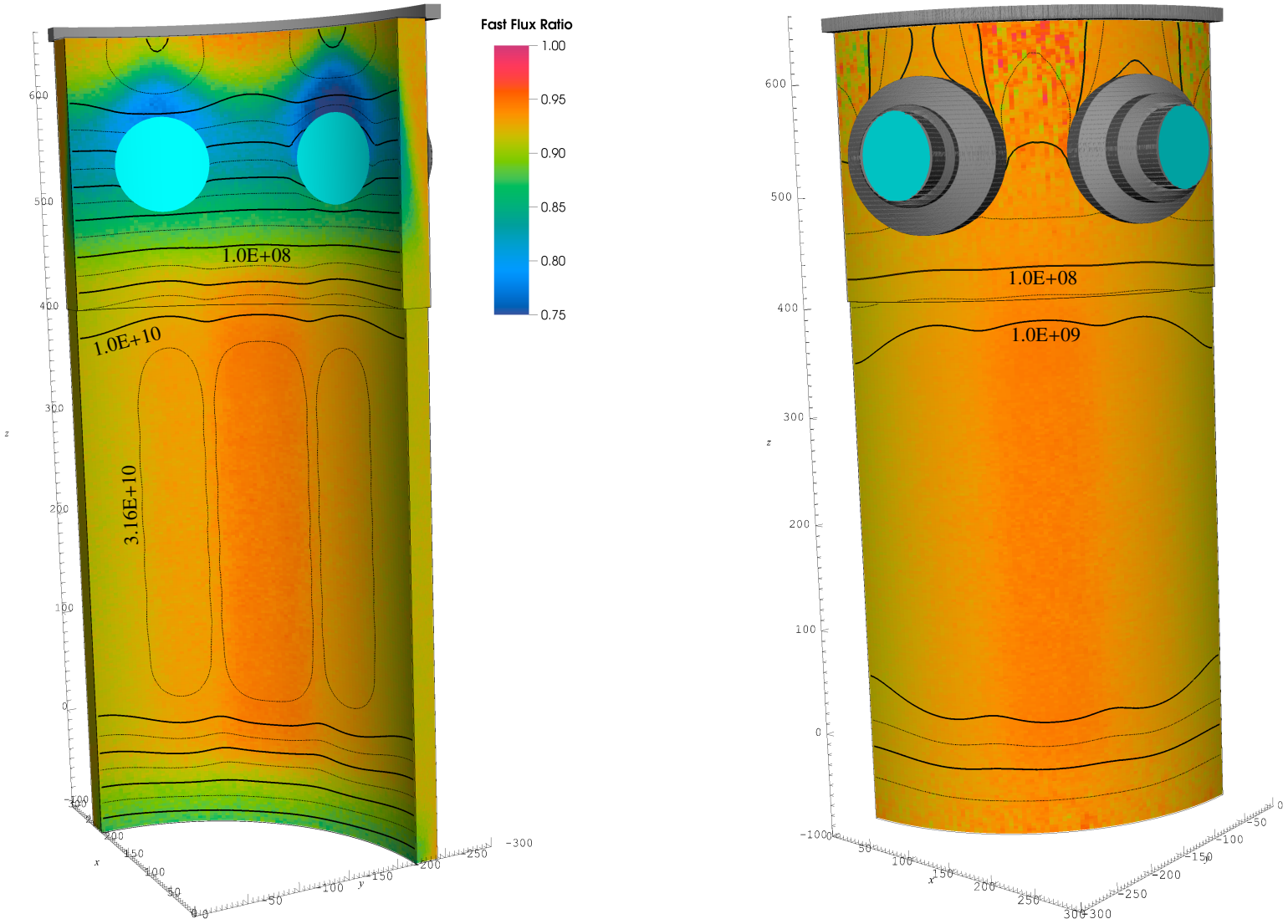

Figure 81. Ratio of the fast neutron flux (E > 1 MeV) on the inner and outer surfaces of the PWR reference model RV when water temperatures in all regions are **decreased by 10 °F**. The core is modeled as a spatially uniform ^{235}U fission source. The cyan regions represent the coolant in the inlet and outlet nozzles. Contour lines correspond to the fast flux for the baseline model. The reduction in flux between each pair of solid contour lines is one decade. Thinner dashed lines are a factor of 3.16 below/above the adjacent solid contours.

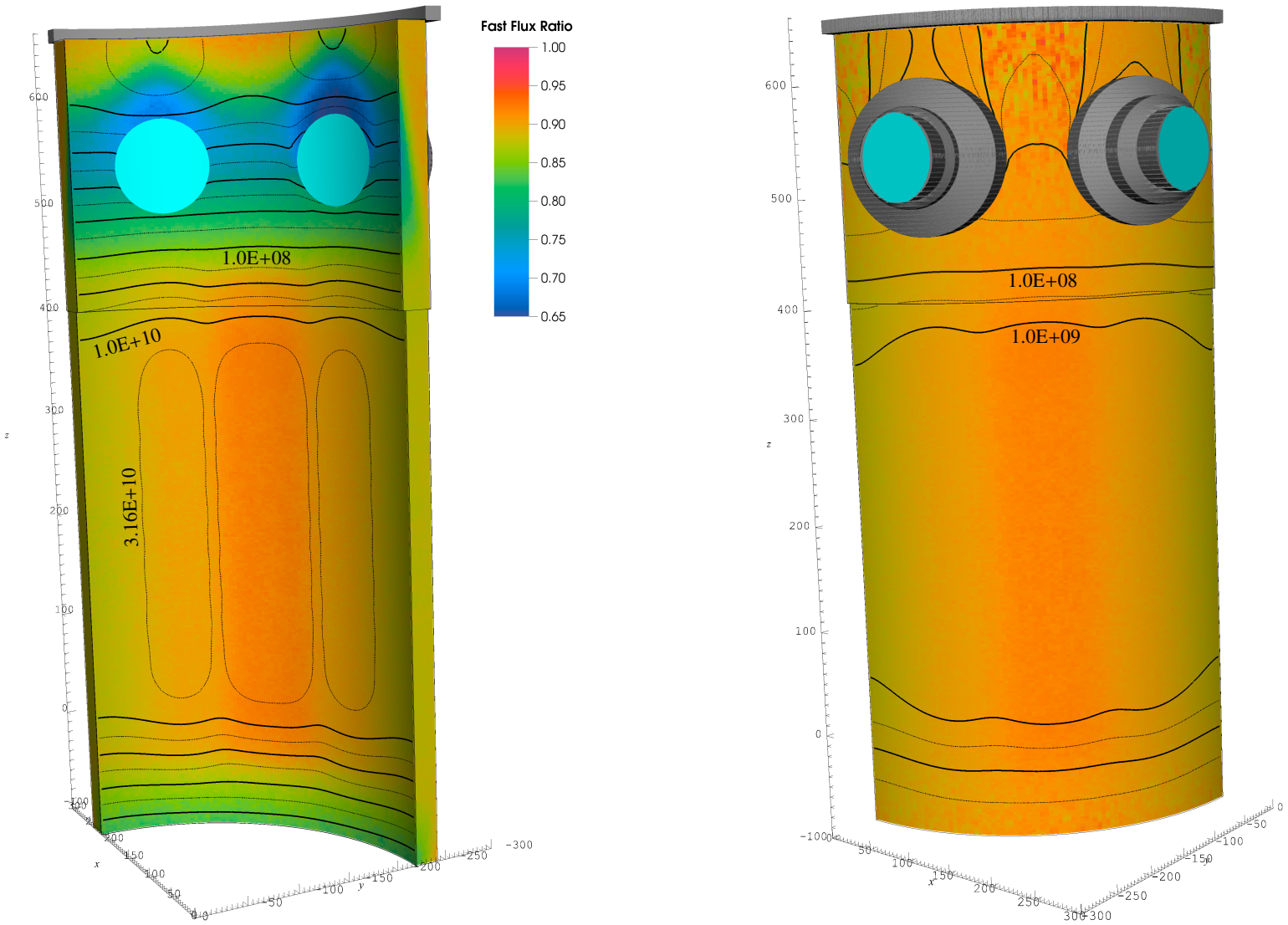

Figure 82. Ratio of the fast neutron flux (E > 1 MeV) on the inner and outer surfaces of the PWR reference model RV when water temperatures in all regions are **decreased by 15 °F**. The core is modeled as a spatially uniform ^{235}U fission source. The cyan regions represent the coolant in the inlet and outlet nozzles. Contour lines correspond to the fast flux for the baseline model. The reduction in flux between each pair of solid contour lines is one decade. Thinner dashed lines are a factor of 3.16 below/above the adjacent solid contours.

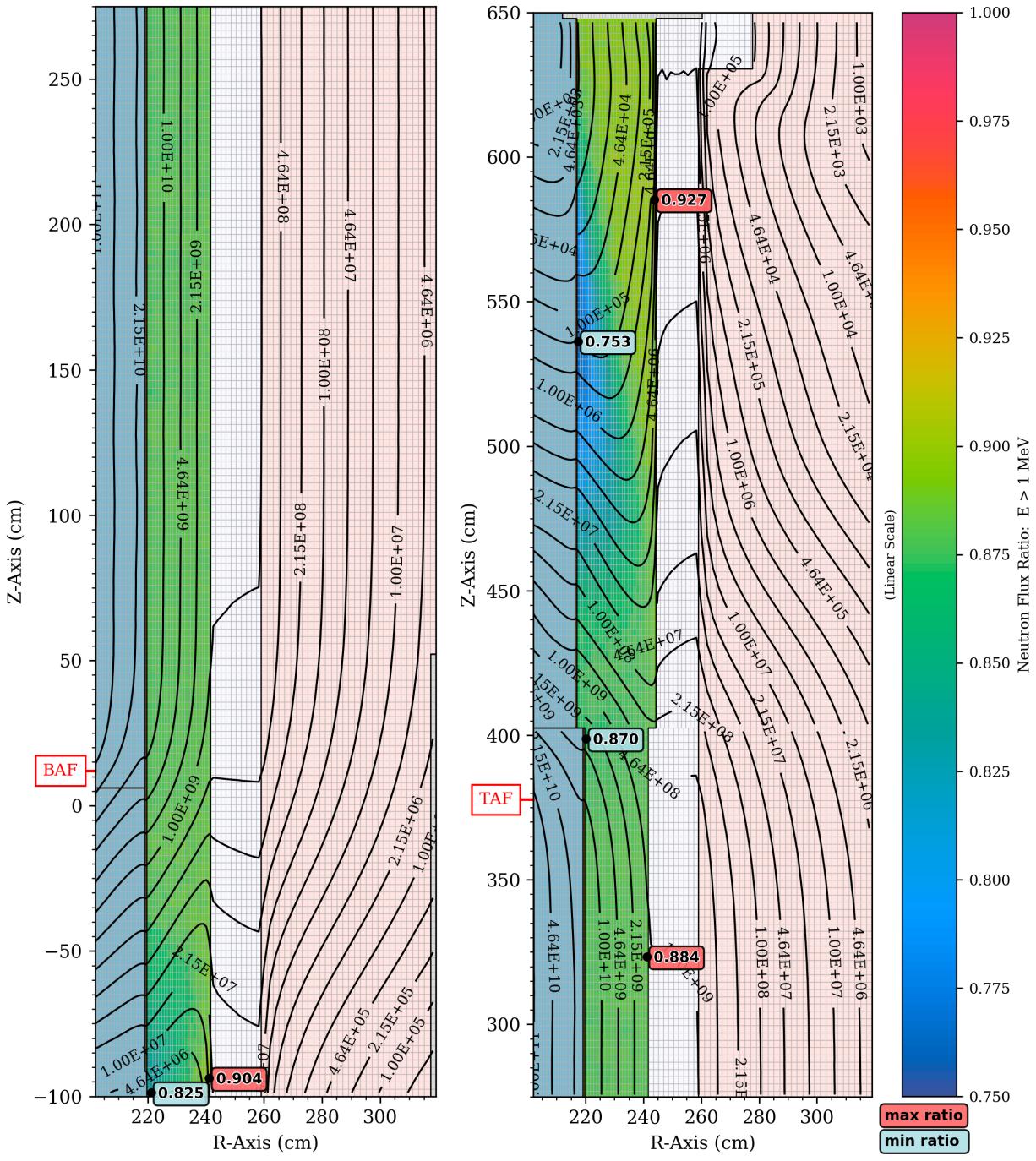

(a) Z = -100 to 275 cm

(b) Z = 275 to 650 cm

Figure 83. Fast neutron flux (E > 1 MeV) in the PWR reference model, and the fast flux ratio when all water temperatures are **decreased by 15 °F**. The core is modeled as a spatially uniform ^{235}U fission source. The elevation view is at **270.5**°, which has the maximum amount of water between the core and the RV. The fast flux ratio in the RV is shown using flooded contours and contour lines. All other regions are colored based on their material assignments. The values inside the shaded boxes are the minimum and maximum ratios in the RV at this azimuthal angle. The minimum and maximum values in (b) are shown separately for the portions of the RV below and above 402.59 cm, where the thickness of the RV changes.

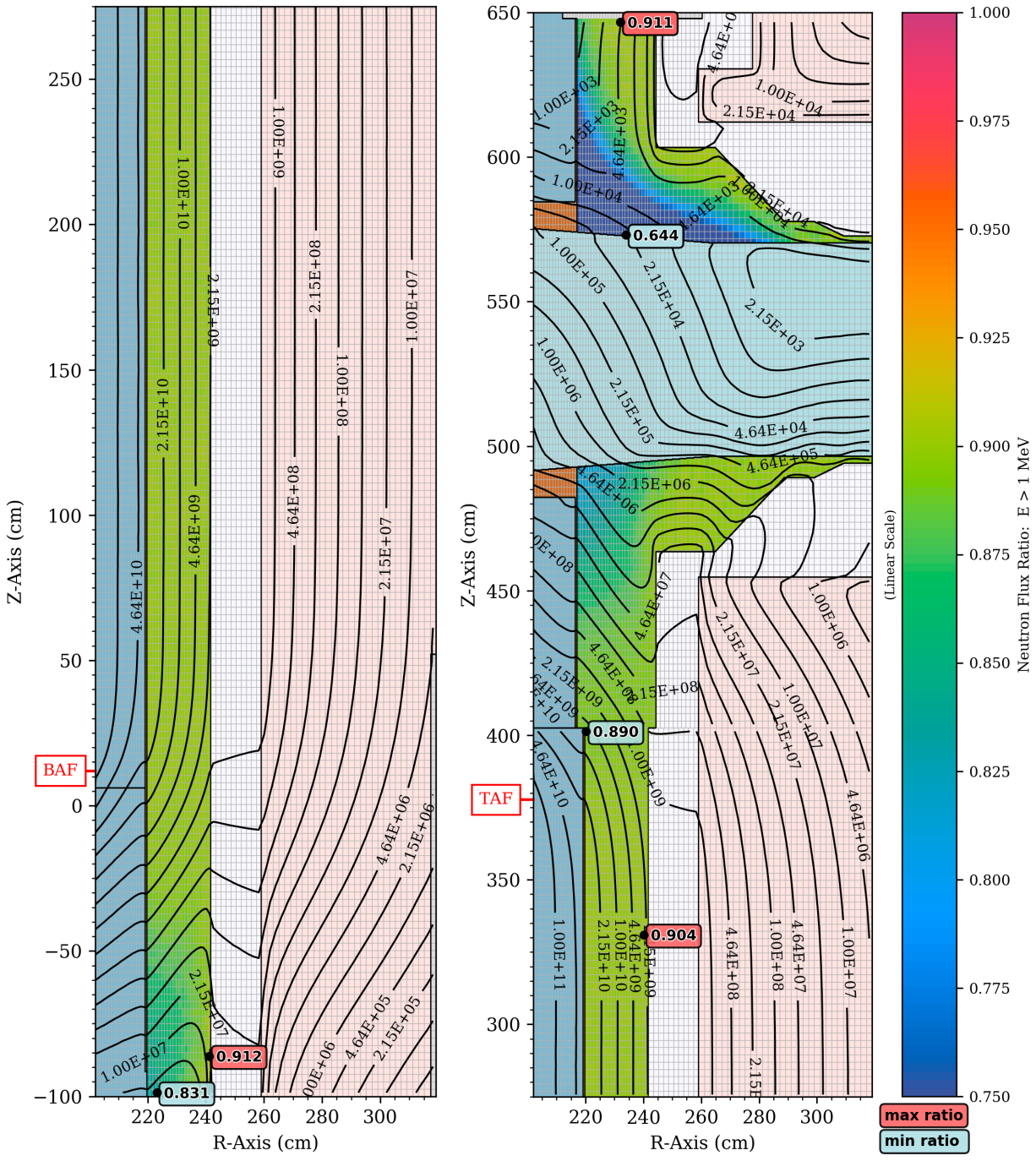

(a) Z = -100 to 275 cm

(b) Z = 275 to 650 cm

Figure 84. Fast neutron flux (E > 1 MeV) in the PWR reference model, and the fast flux ratio when all water temperatures are **decreased by 15 °F**. The core is modeled as a spatially uniform ^{235}U fission source. The elevation view is at **292.5**°, which is the centerline of the outlet nozzle. The fast flux ratio in the RV and the nozzles is shown using flooded contours and contour lines. All other regions are colored based on their material assignments. The values inside the shaded boxes are the minimum and maximum ratios in the RV and the nozzles at this azimuthal angle. The minimum and maximum values in (b) are shown separately for the portions of the RV below and above 402.59 cm, where the thickness of the RV changes.

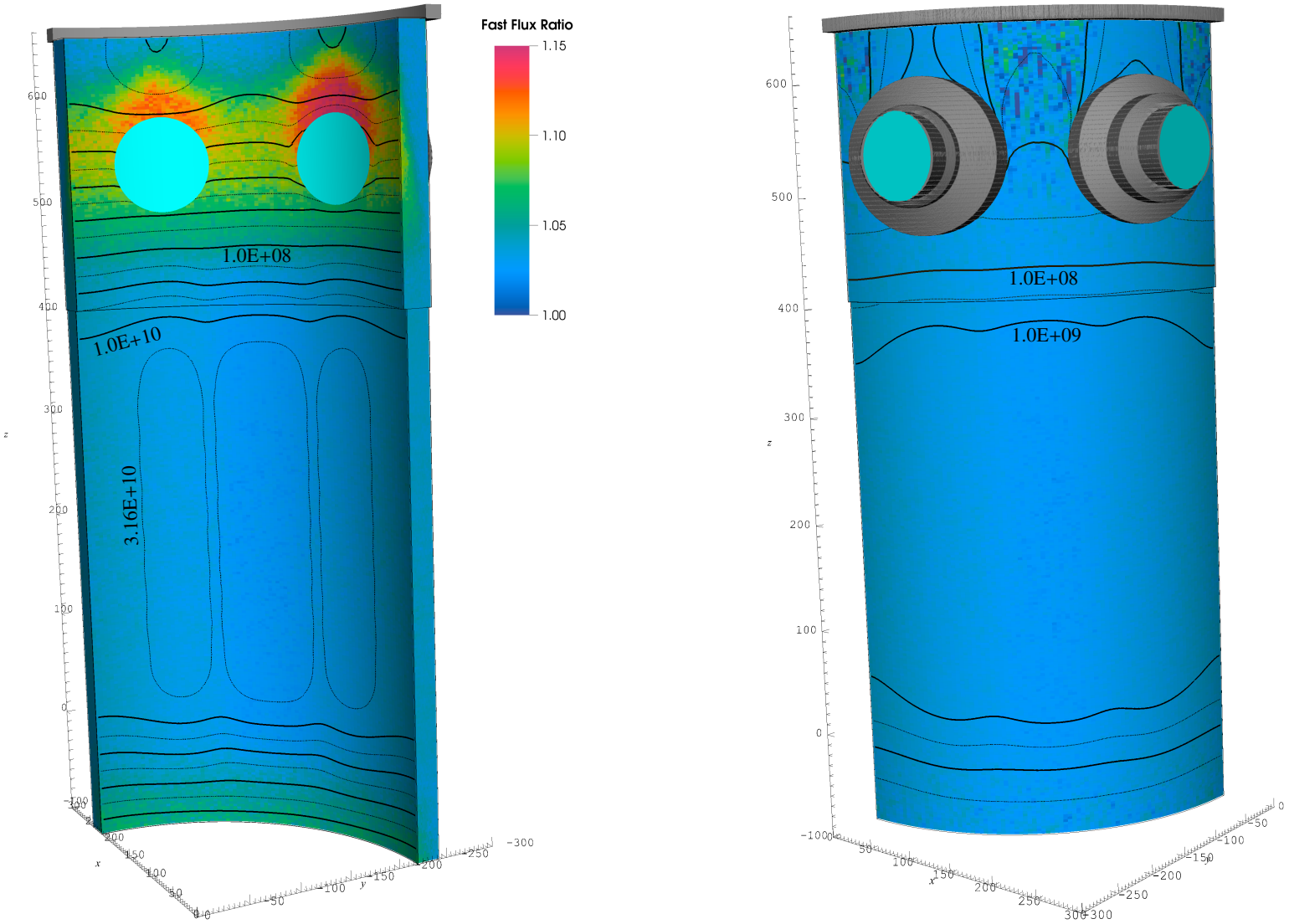

Figure 85. Ratio of the fast neutron flux (E > 1 MeV) on the inner and outer surfaces of the PWR reference model RV when water temperatures in all regions are **increased by 5 °F**. The core is modeled as a spatially uniform ^{235}U fission source. The cyan regions represent the coolant in the inlet and outlet nozzles. Contour lines correspond to the fast flux for the baseline model. The reduction in flux between each pair of solid contour lines is one decade. Thinner dashed lines are a factor of 3.16 below/above the adjacent solid contours.

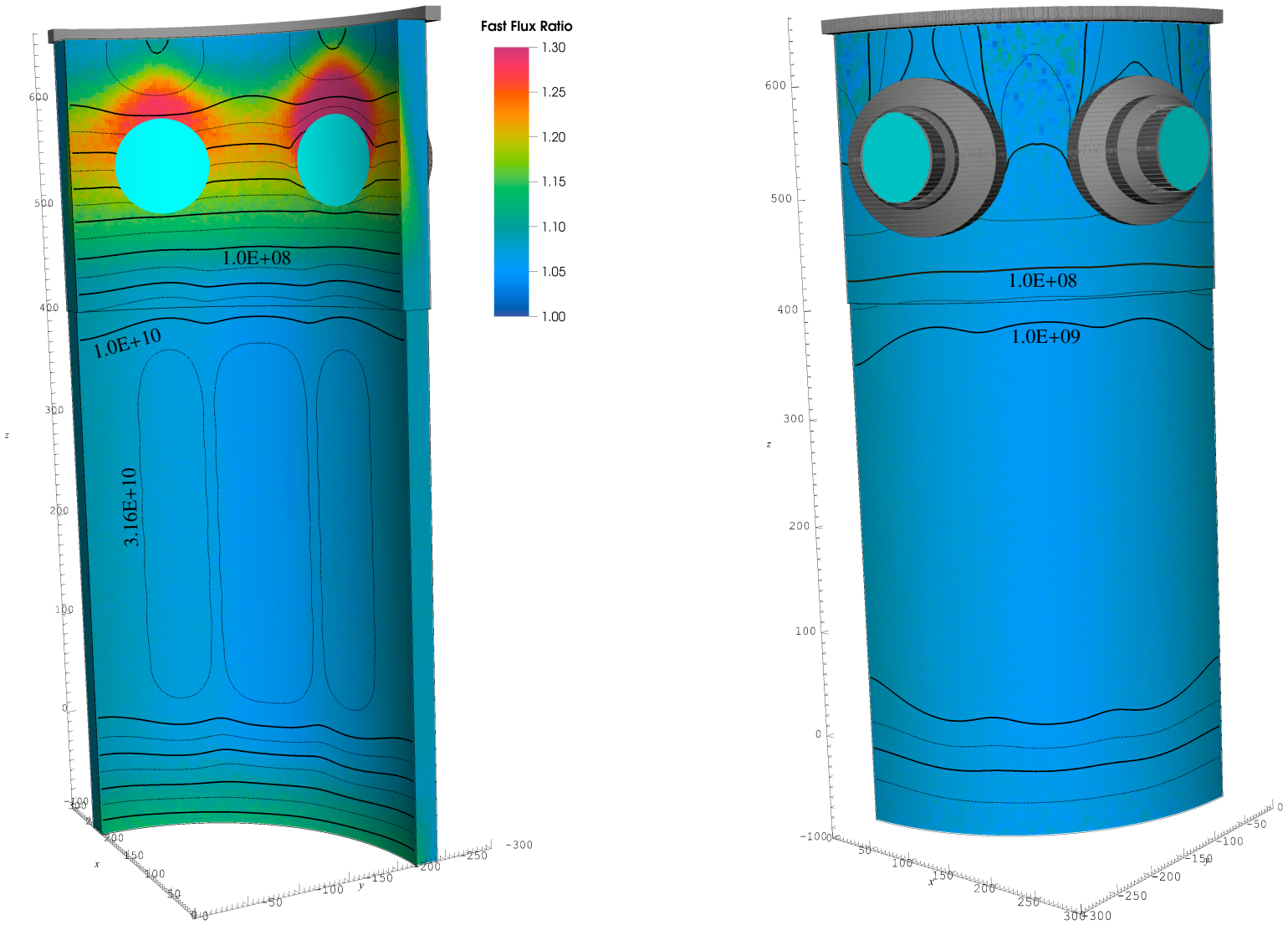

Figure 86. Ratio of the fast neutron flux (E > 1 MeV) on the inner and outer surfaces of the PWR reference model RV when water temperatures in all regions are **increased by 10 °F**. The core is modeled as a spatially uniform ^{235}U fission source. The cyan regions represent the coolant in the inlet and outlet nozzles. Contour lines correspond to the fast flux for the baseline model. The reduction in flux between each pair of solid contour lines is one decade. Thinner dashed lines are a factor of 3.16 below/above the adjacent solid contours.

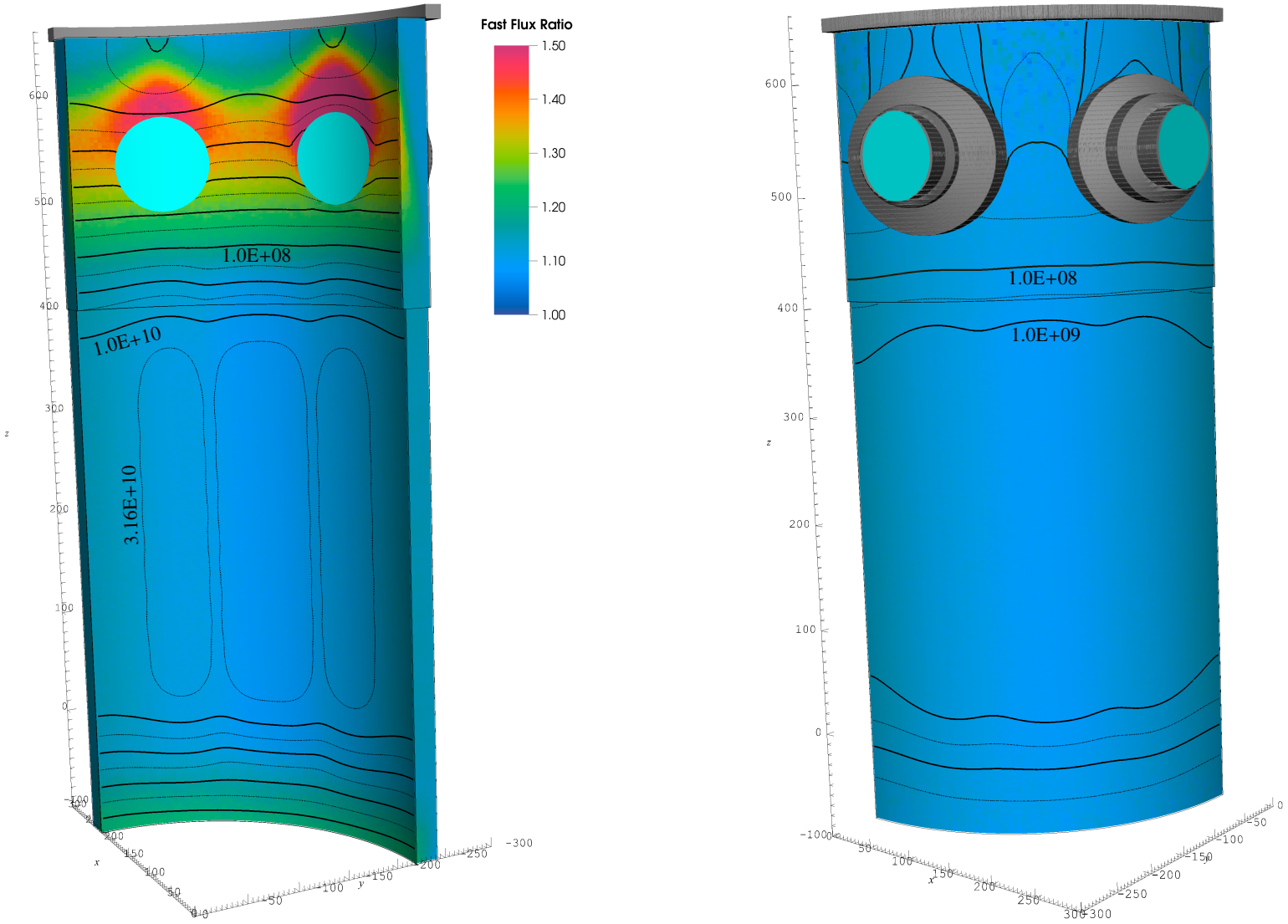

Figure 87. Ratio of the fast neutron flux (E > 1 MeV) on the inner and outer surfaces of the PWR reference model RV when water temperatures in all regions are **increased by 15 °F**. The core is modeled as a spatially uniform ^{235}U fission source. The cyan regions represent the coolant in the inlet and outlet nozzles. Contour lines correspond to the fast flux for the baseline model. The reduction in flux between each pair of solid contour lines is one decade. Thinner dashed lines are a factor of 3.16 below/above the adjacent solid contours.

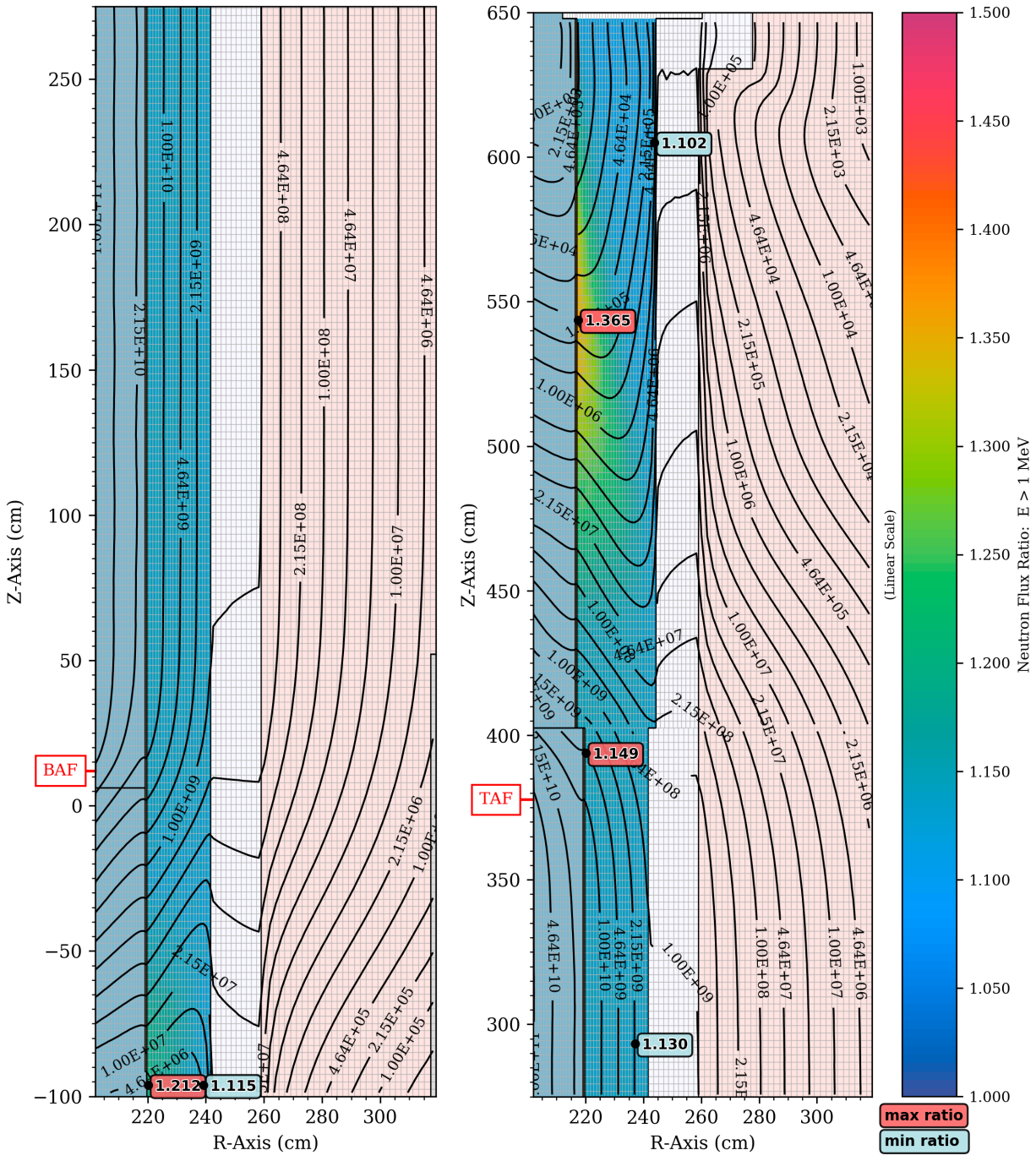

(a) Z = -100 to 275 cm

(b) Z = 275 to 650 cm

Figure 88. Fast neutron flux (E > 1 MeV) in the PWR reference model, and the fast flux ratio when all water temperatures are **increased by 15 °F**. The core is modeled as a spatially uniform ^{235}U fission source. The elevation view is at **270.5**°, which has the maximum amount of water between the core and the RV. The fast flux ratio in the RV is shown using flooded contours and contour lines. All other regions are colored based on their material assignments. The values inside the shaded boxes are the minimum and maximum ratios in the RV at this azimuthal angle. The minimum and maximum values in (b) are shown separately for the portions of the RV below and above 402.59 cm, where the thickness of the RV changes.

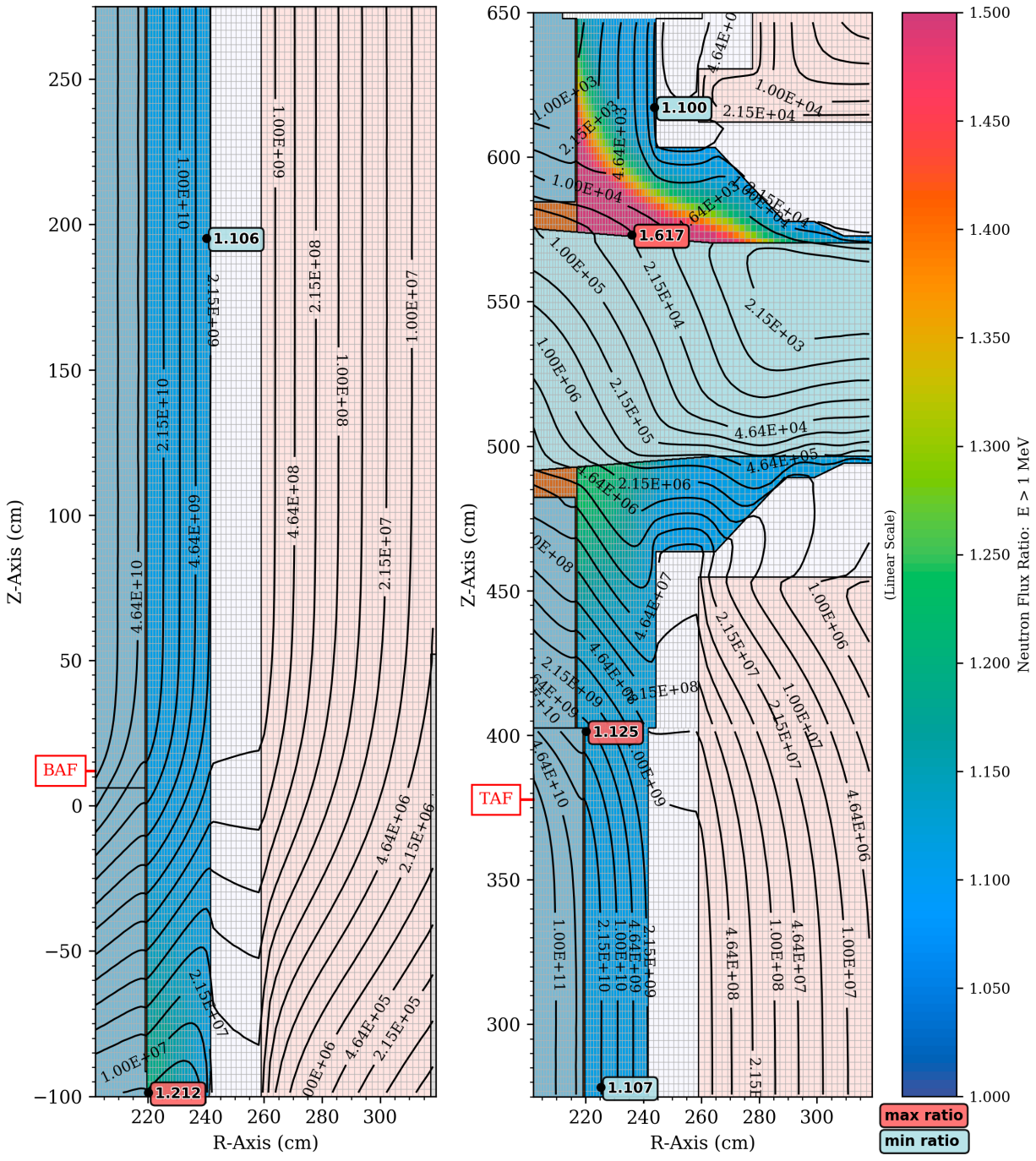

(a) Z = -100 to 275 cm

(b) Z = 275 to 650 cm

Figure 89. Fast neutron flux (E > 1 MeV) in the PWR reference model, and the fast flux ratio when all water temperatures are **increased by 15 °F**. The core is modeled as a spatially uniform ^{235}U fission source. The elevation view is at **292.5**°, which is the centerline of the outlet nozzle. The fast flux ratio in the RV and the nozzles is shown using flooded contours and contour lines. All other regions are colored based on their material assignments. The values inside the shaded boxes are the minimum and maximum ratios in the RV and the nozzles at this azimuthal angle. The minimum and maximum values in (b) are shown separately for the portions of the RV below and above 402.59 cm, where the thickness of the RV changes.

8 Homogenized Metal/Water Core Plates and Top and Bottom Nozzle Parameter Study

In the creation of the PWR reference model, exact details of the top and bottom core plates and the top and bottom nozzles on each fuel assembly were not available. Because of this, these regions were modeled as metal/water (M/W) regions based on the best available modeling information.

These reactor vessel internal structures have essentially no effect on the fast neutron flux levels in the RV within the active fuel height. However, they may be important for RV locations outside that region. To assess the potential impact, a parametric study was run in which the density of the metal/water regions representing the core plates and assembly nozzles was increased or decreased by 10% and 25%.

The results of these parameter changes are shown in Figures 90–92 for M/W density reductions of 10%; Figures 93–95 for M/W density increases of 10%; Figures 96–98 for M/W density reductions of 25%; and Figures 99–101 for M/W density increases of 25%.

Within the portion of the RV that is at elevations within the active fuel height, there is, as expected, essentially no effect on RV fluence as the density of the homogenized metal/water regions is changed. At locations outside the 'traditional' beltline region, the fast flux levels change by as much as ~70% for the density variations considered in this analysis. The location where the greatest changes occur are near the bottom of the cylindrical portion of the RV (i.e., just above the lower head) and at elevations near the inlet and outlet nozzles. This behavior is consistent with the results of adjoint neutron flux calculations that are presented in Section 12.

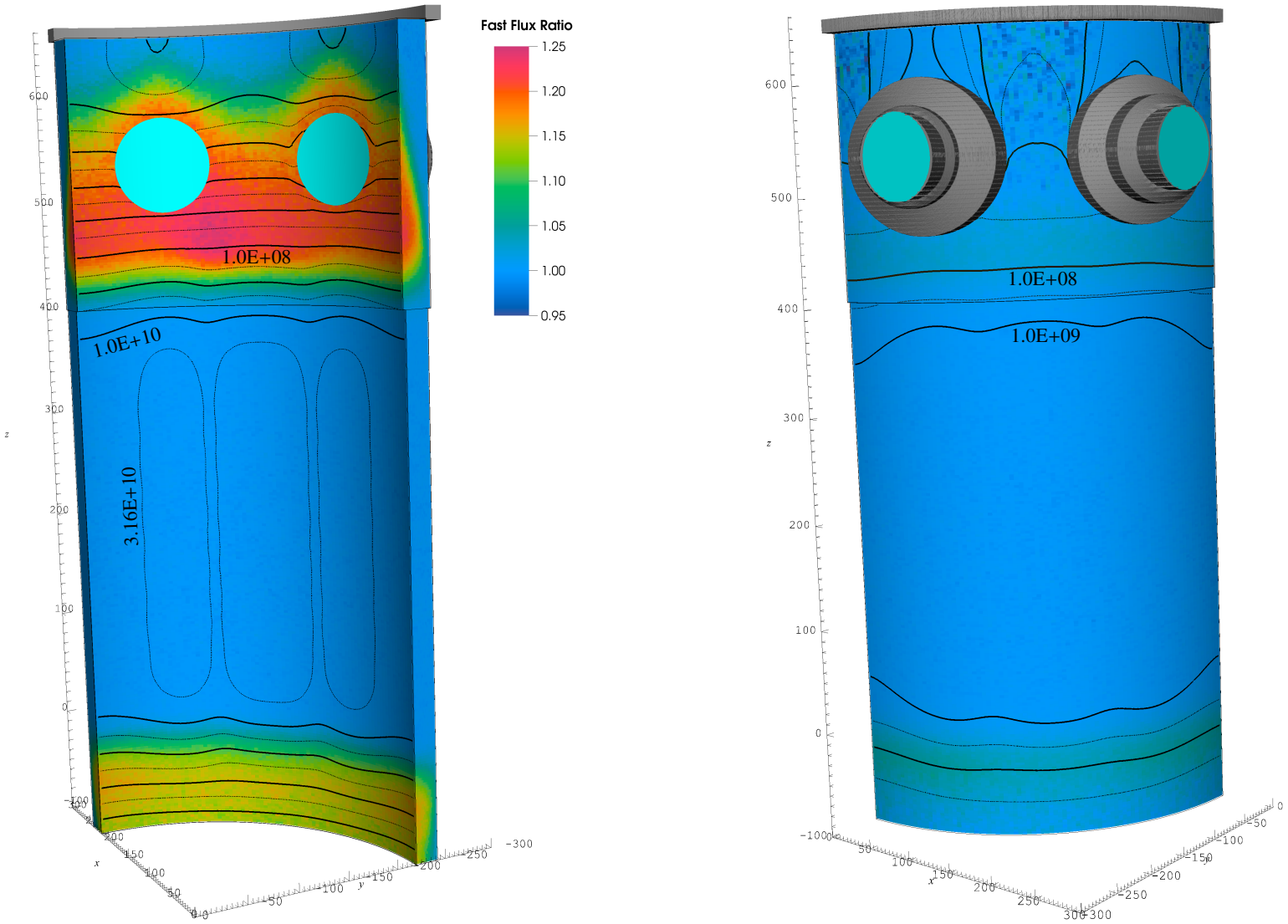

Figure 90. Ratio of the neutron flux (E > 1 MeV) on the inner and outer surfaces of the PWR reference model RV when the densities of the metal/water regions for the core plates and top and bottom assembly nozzles are **decreased by 10%**. The core is modeled as a spatially uniform ^{235}U fission source. The cyan regions represent the coolant in the inlet and outlet nozzles. The contour lines correspond to the fast flux for the baseline model. The reduction in flux between each pair of solid contour lines is one decade. The thinner dashed lines are a factor of 3.16 below/above the adjacent solid contours.

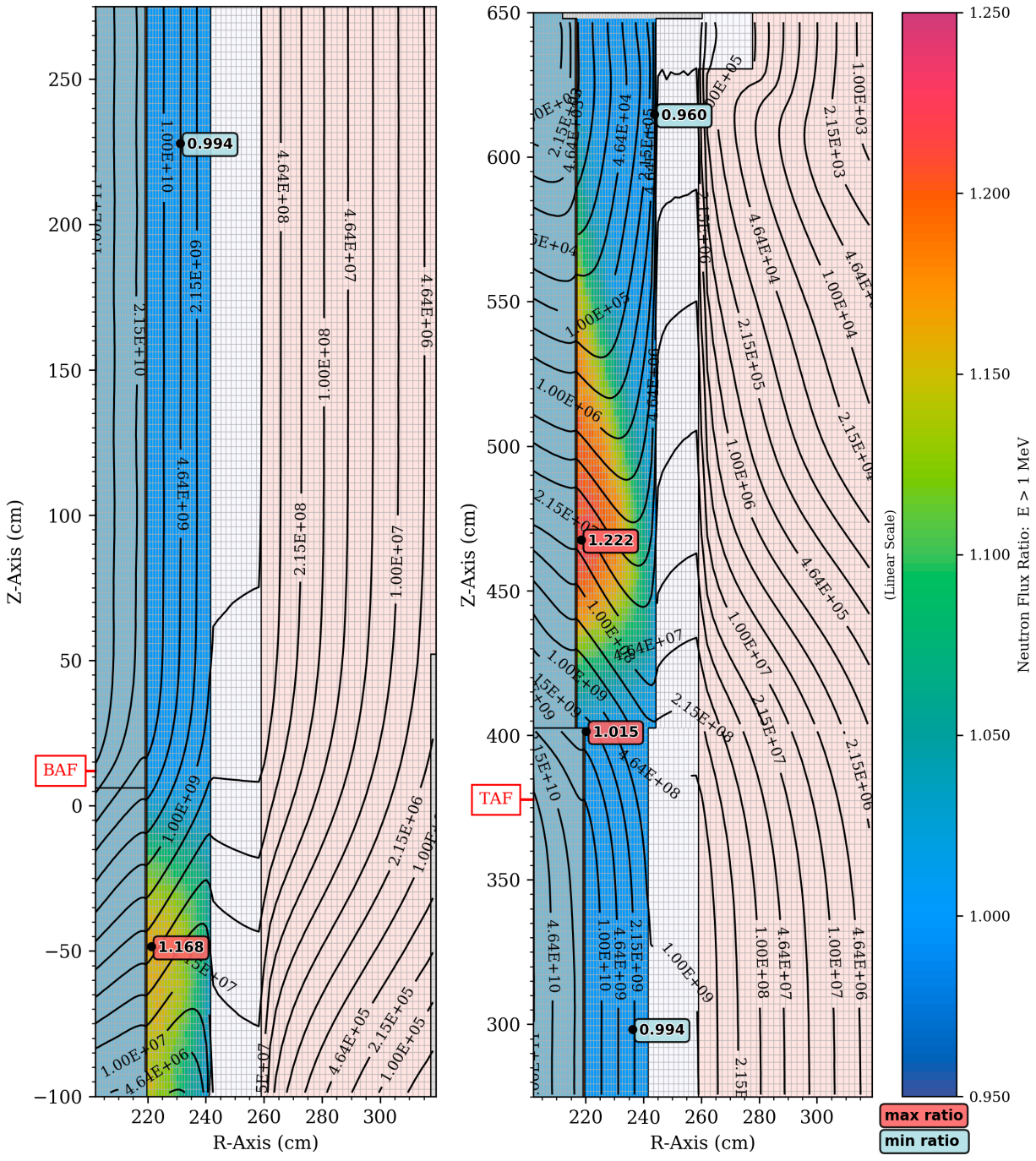

(a) Z = -100 to 275 cm

(b) Z = 275 to 650 cm

Figure 91. Fast neutron flux (E > 1 MeV) in the PWR reference model, and the flux ratio when the densities of the metal/water regions for the core plates and top and bottom assembly nozzles are **decreased by 10%**. The core is modeled as a spatially uniform ^{235}U fission source. The elevation view is at **270.5**°, which has the maximum amount of water between the core and the RV. The fast flux ratio in the RV is shown using flooded contours and contour lines. All other regions are colored based on their material assignments. The values inside the shaded boxes are the minimum and maximum ratios in the RV at this azimuthal angle. The minimum and maximum values in (b) are shown separately for the portions of the RV below and above 402.59 cm, where the thickness of the RV changes.

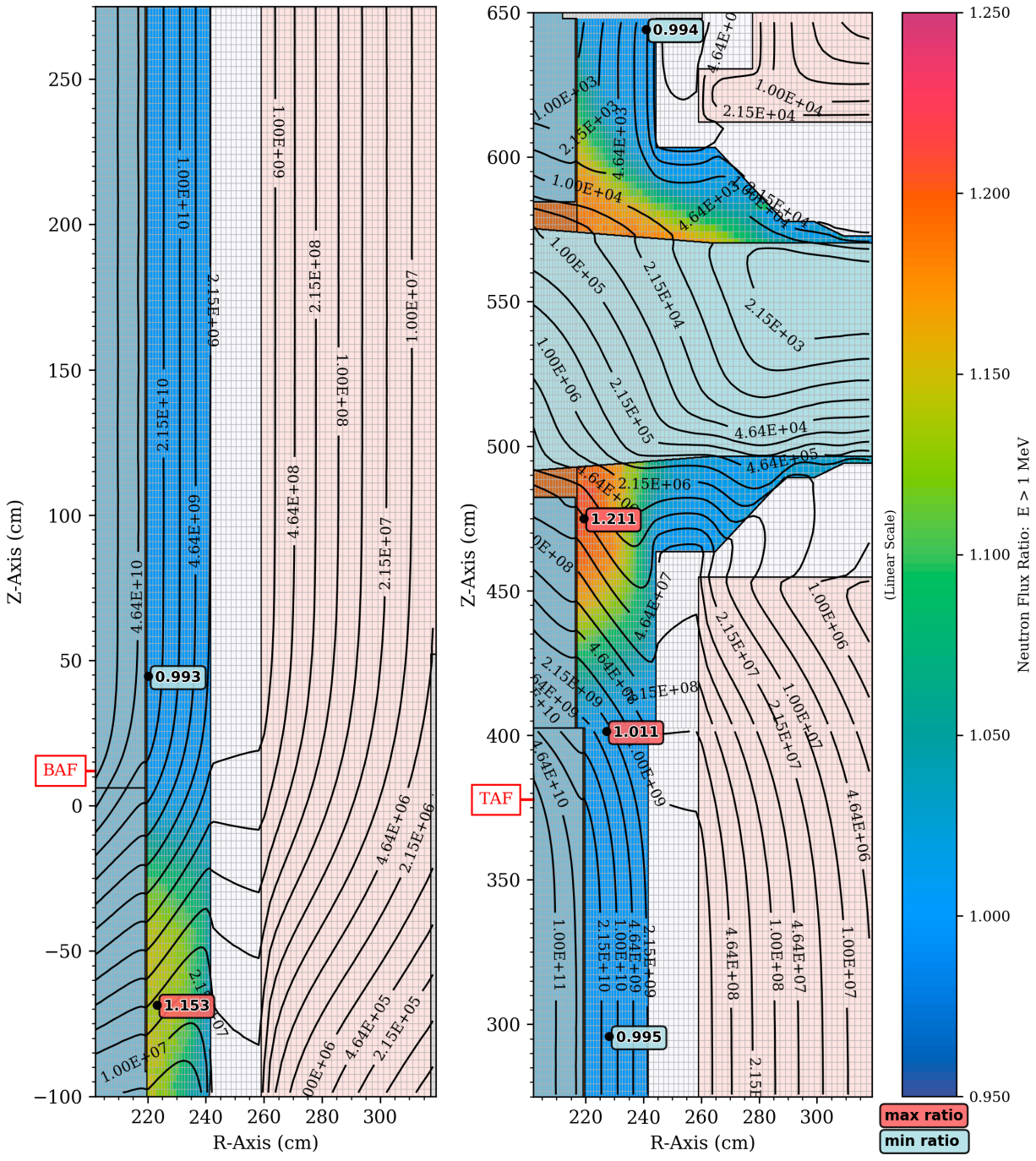

(a) Z = -100 to 275 cm

(b) Z = 275 to 650 cm

Figure 92. Fast neutron flux (E > 1 MeV) in the PWR reference model, and the flux ratio when the densities of the metal/water regions for the core plates and top and bottom assembly nozzles are **decreased by 10%**. The core is modeled as a spatially uniform ^{235}U fission source. The elevation view is at **292.5**°, the location of the outlet nozzle. The fast flux ratio in the RV and the nozzle is shown using flooded contours and contour lines. All other regions are colored based on their material assignments. The values inside the shaded boxes are the minimum and maximum ratios in the RV and the nozzle at this azimuthal angle. The minimum and maximum values in (b) are shown separately for the portions of the RV below and above 402.59 cm, where the thickness of the RV changes.

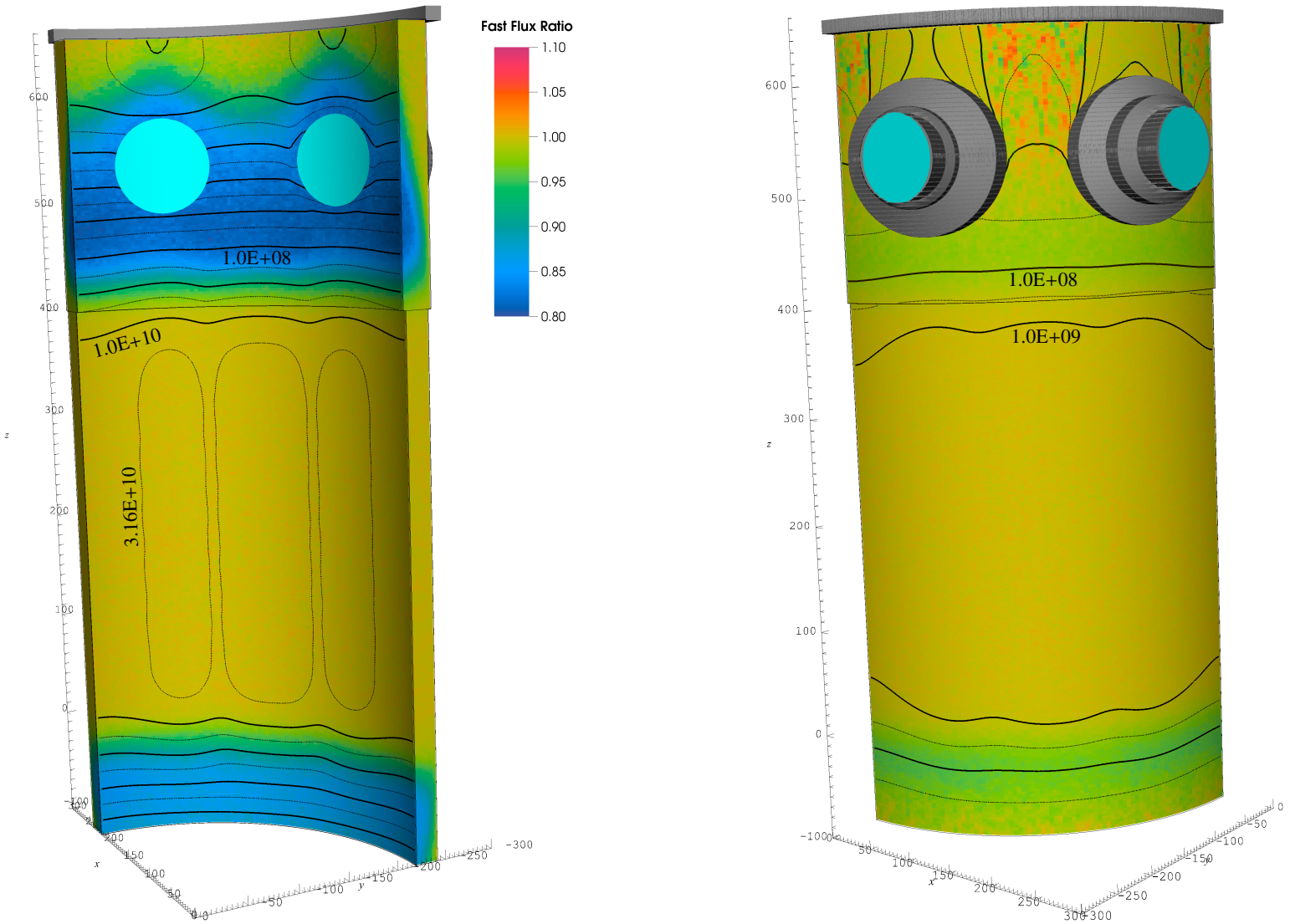

Figure 93. Ratio of the neutron flux (E > 1 MeV) on the inner and outer surfaces of the PWR reference model RV when the densities of the metal/water regions for the core plates and top and bottom assembly nozzles are **increased by 10%**. The core is modeled as a spatially uniform ^{235}U fission source. The cyan regions represent the coolant in the inlet and outlet nozzles. The contour lines correspond to the fast flux for the baseline model. The reduction in flux between each pair of solid contour lines is one decade. The thinner dashed lines are a factor of 3.16 below/above the adjacent solid contours.

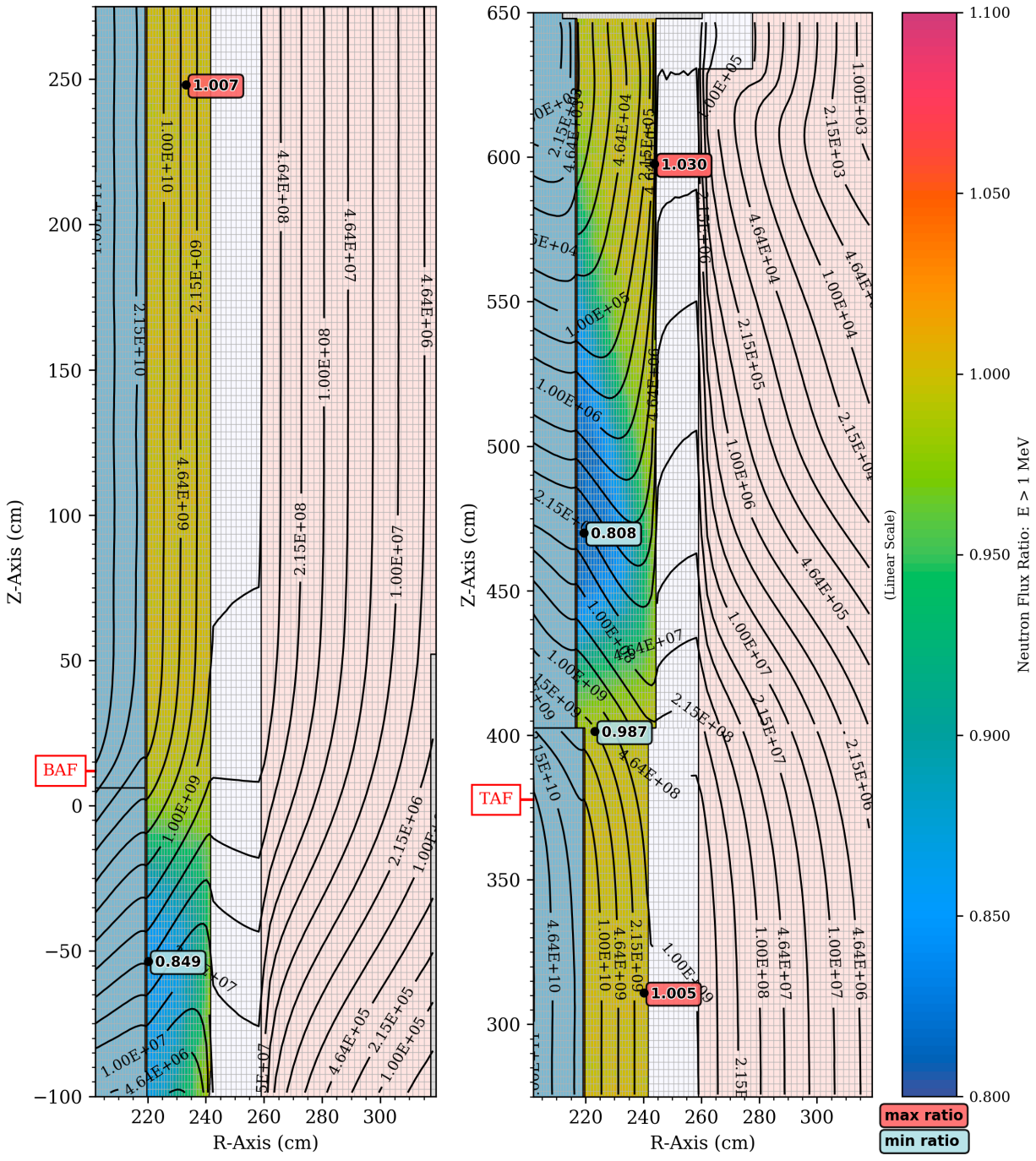

(a) Z = -100 to 275 cm

(b) Z = 275 to 650 cm

Figure 94. Fast neutron flux (E > 1 MeV) in the PWR reference model, and the flux ratio when the densities of the metal/water regions for the core plates and top and bottom assembly nozzles are **increased by 10%**. The core is modeled as a spatially uniform ^{235}U fission source. The elevation view is at **270.5**°, which has the maximum amount of water between the core and the RV. The fast flux ratio in the RV is shown using flooded contours and contour lines. All other regions are colored based on their material assignments. The values inside the shaded boxes are the minimum and maximum ratios in the RV at this azimuthal angle. The minimum and maximum values in (b) are shown separately for the portions of the RV below and above 402.59 cm, where the thickness of the RV changes.

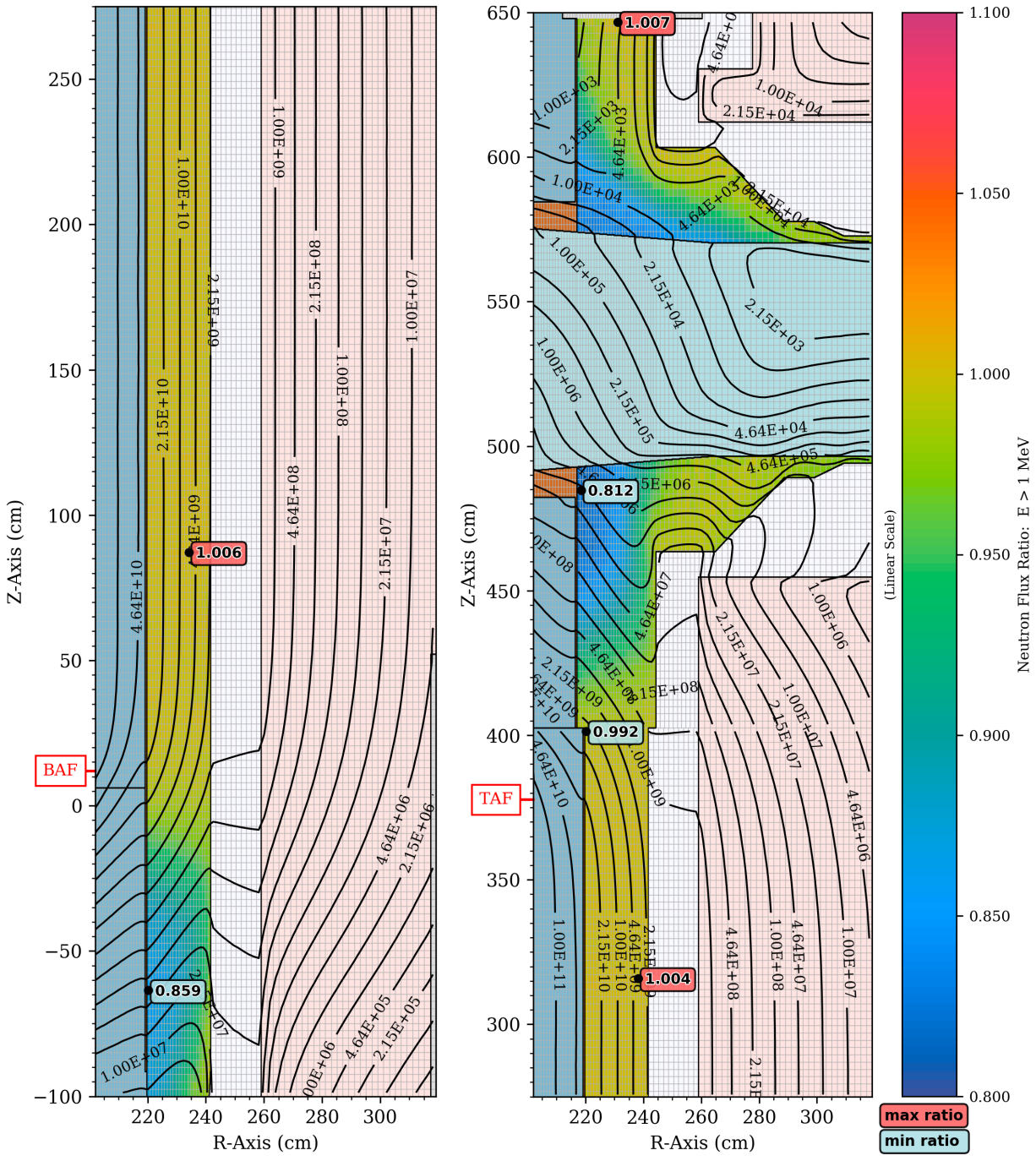

(a) Z = -100 to 275 cm

(b) Z = 275 to 650 cm

Figure 95. Fast neutron flux (E > 1 MeV) in the PWR reference model, and the flux ratio when the densities of the metal/water regions for the core plates and top and bottom assembly nozzles are **increased by 10%**. The core is modeled as a spatially uniform ^{235}U fission source. The elevation view is at **292.5**°, the location of the outlet nozzle. The fast flux ratio in the RV and the nozzle is shown using flooded contours and contour lines. All other regions are colored based on their material assignments. The values inside the shaded boxes are the minimum and maximum ratios in the RV and the nozzle at this azimuthal angle. The minimum and maximum values in (b) are shown separately for the portions of the RV below and above 402.59 cm, where the thickness of the RV changes.

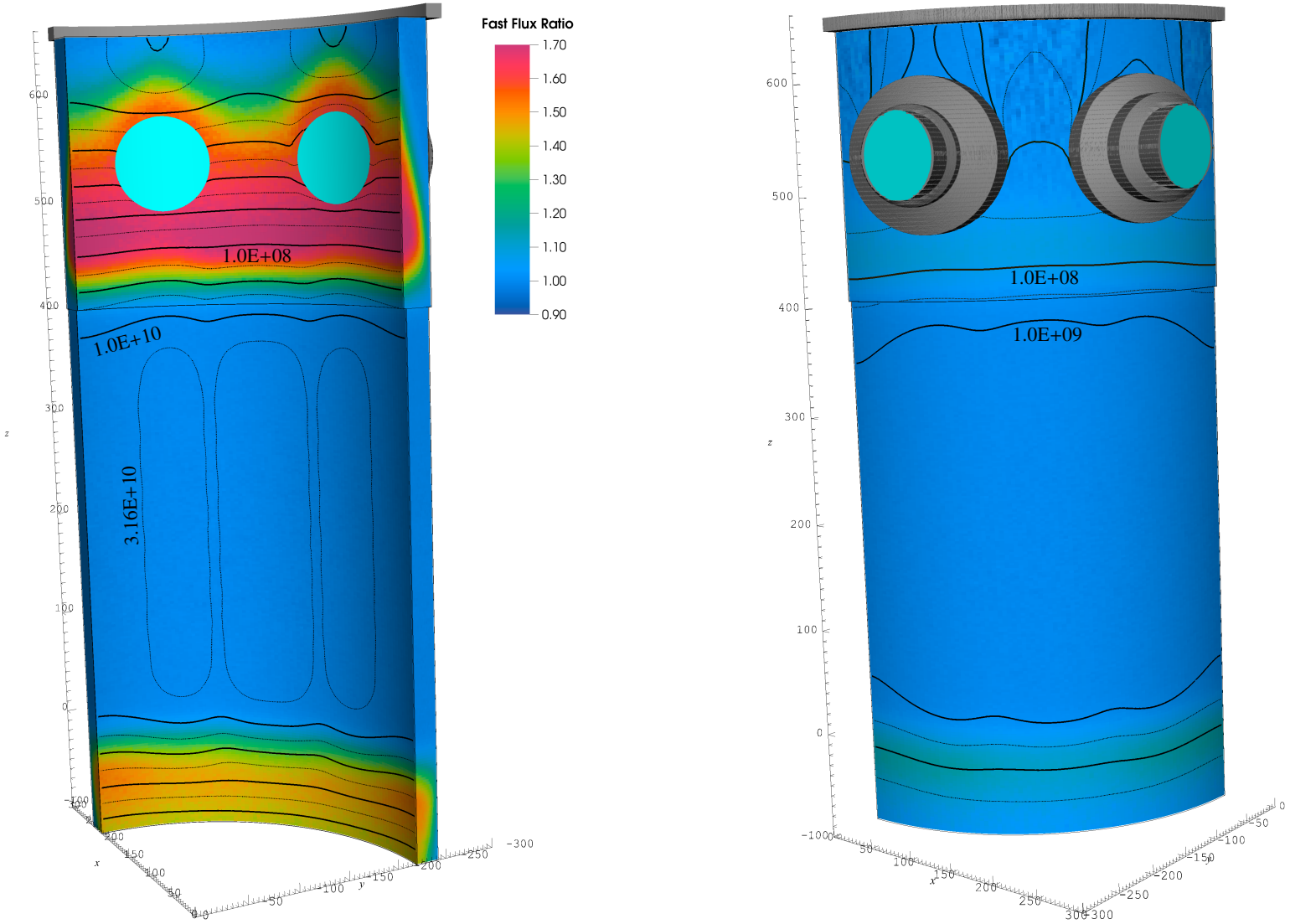

Figure 96. Ratio of the neutron flux (E > 1 MeV) on the inner and outer surfaces of the PWR reference model RV when the densities of the metal/water regions for the core plates and top and bottom assembly nozzles are **decreased by 25%**. The core is modeled as a spatially uniform ^{235}U fission source. The cyan regions represent the coolant in the inlet and outlet nozzles. The contour lines correspond to the fast flux for the baseline model. The reduction in flux between each pair of solid contour lines is one decade. The thinner dashed lines are a factor of 3.16 below/above the adjacent solid contours.

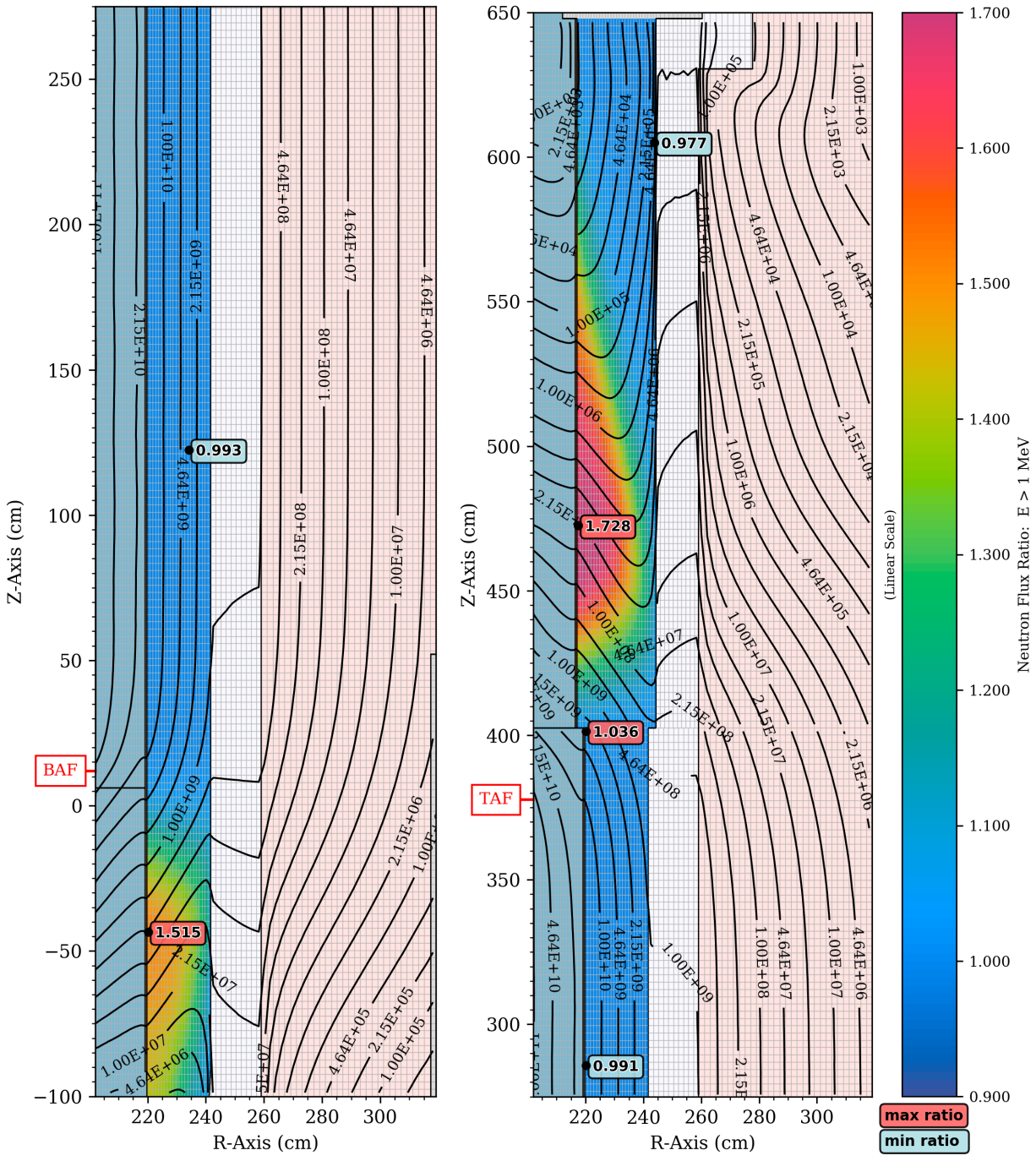

(a) Z = -100 to 275 cm

(b) Z = 275 to 650 cm

Figure 97. Fast neutron flux (E > 1 MeV) in the PWR reference model, and the flux ratio when the densities of the metal/water regions for the core plates and top and bottom assembly nozzles are **decreased by 25%**. The core is modeled as a spatially uniform ^{235}U fission source. The elevation view is at **270.5**°, which has the maximum amount of water between the core and the RV. The fast flux ratio in the RV is shown using flooded contours and contour lines. All other regions are colored based on their material assignments. The values inside the shaded boxes are the minimum and maximum ratios in the RV at this azimuthal angle. The minimum and maximum values in (b) are shown separately for the portions of the RV below and above 402.59 cm, where the thickness of the RV changes.

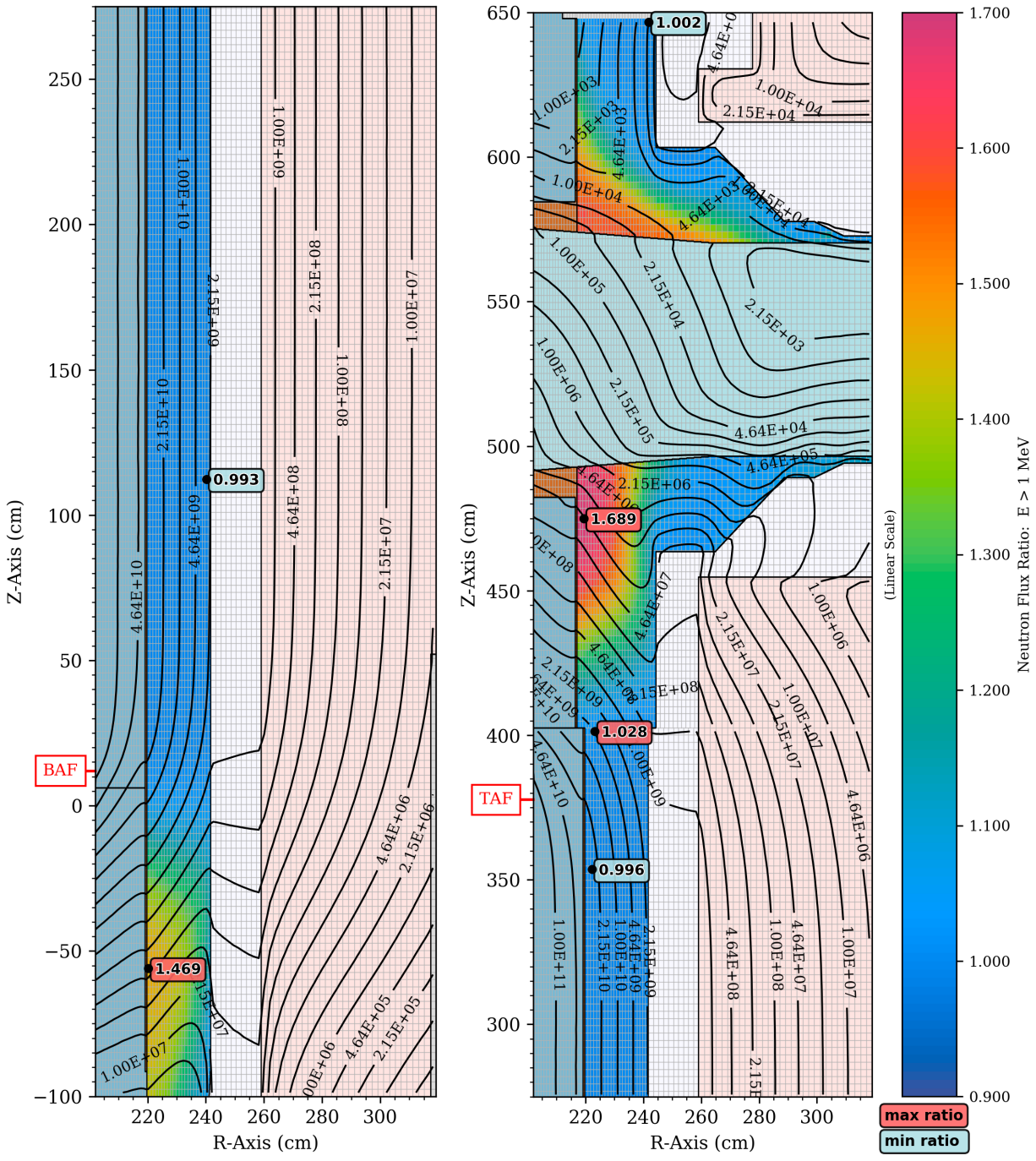

(a) Z = -100 to 275 cm

(b) Z = 275 to 650 cm

Figure 98. Fast neutron flux (E > 1 MeV) in the PWR reference model, and the flux ratio when the densities of the metal/water regions for the core plates and top and bottom assembly nozzles are **decreased by 25%**. The core is modeled as a spatially uniform ^{235}U fission source. The elevation view is at **292.5**°, the location of the outlet nozzle. The fast flux ratio in the RV and the nozzle is shown using flooded contours and contour lines. All other regions are colored based on their material assignments. The values inside the shaded boxes are the minimum and maximum ratios in the RV and the nozzle at this azimuthal angle. The minimum and maximum values in (b) are shown separately for the portions of the RV below and above 402.59 cm, where the thickness of the RV changes.

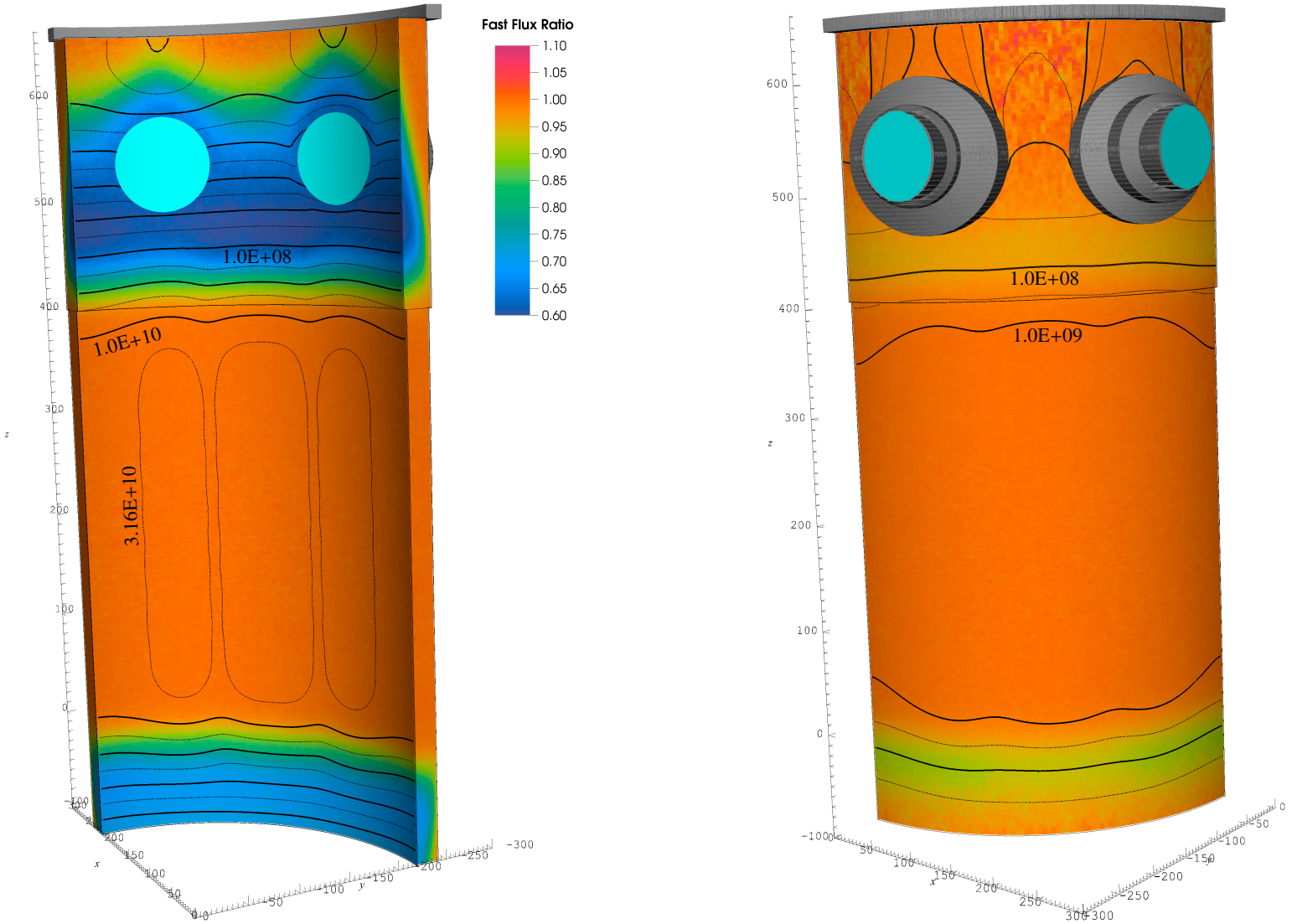

Figure 99. Ratio of the neutron flux (E > 1 MeV) on the inner and outer surfaces of the PWR reference model RV when the densities of the metal/water regions for the core plates and top and bottom assembly nozzles are **increased by 25%**. The core is modeled as a spatially uniform ^{235}U fission source. The cyan regions represent the coolant in the inlet and outlet nozzles. The contour lines correspond to the fast flux for the baseline model. The reduction in flux between each pair of solid contour lines is one decade. The thinner dashed lines are a factor of 3.16 below/above the adjacent solid contours.

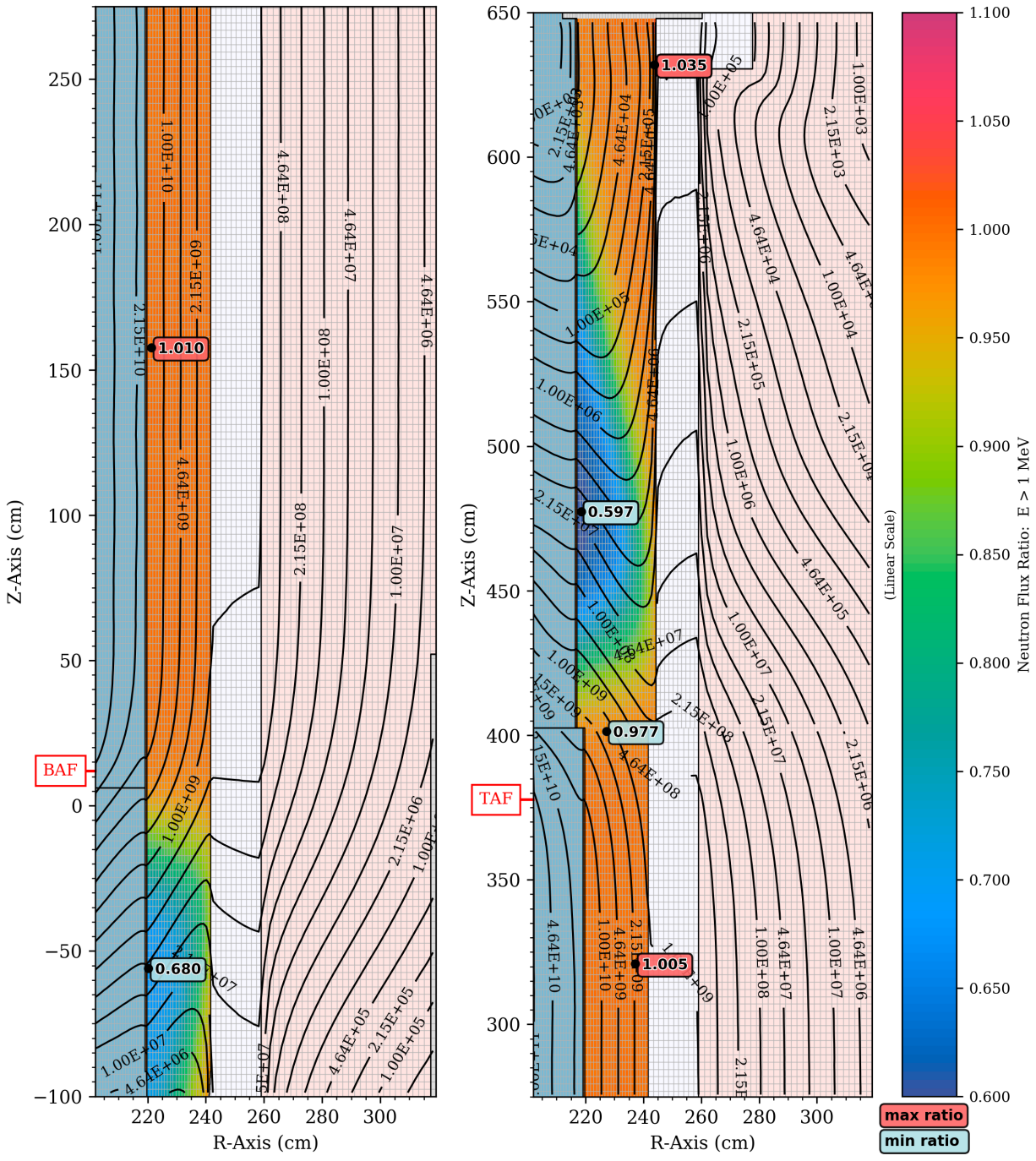

(a) Z = -100 to 275 cm

(b) Z = 275 to 650 cm

Figure 100. Fast neutron flux (E > 1 MeV) in the PWR reference model, and the flux ratio when the densities of the metal/water regions for the core plates and top and bottom assembly nozzles are **increased by 25%**. The core is modeled as a spatially uniform ^{235}U fission source. The elevation view is at **270.5**°, which has the maximum amount of water between the core and the RV. The fast flux ratio in the RV is shown using flooded contours and contour lines. All other regions are colored based on their material assignments. The values inside the shaded boxes are the minimum and maximum ratios in the RV at this azimuthal angle. The minimum and maximum values in (b) are shown separately for the portions of the RV below and above 402.59 cm, where the thickness of the RV changes.

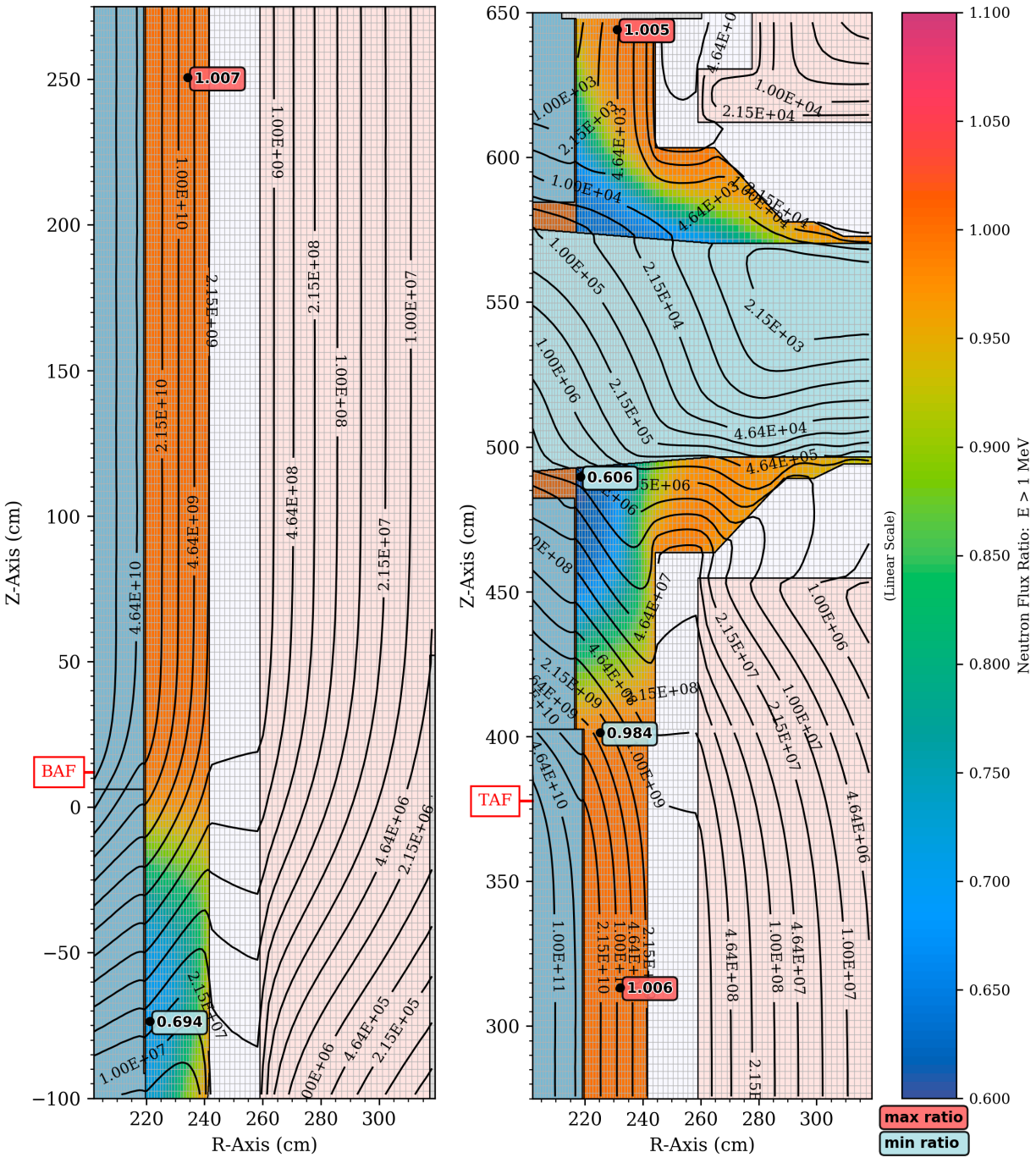

(a) Z = -100 to 275 cm

(b) Z = 275 to 650 cm

Figure 101. Fast neutron flux (E > 1 MeV) in the PWR reference model, and the flux ratio when the densities of the metal/water regions for the core plates and top and bottom assembly nozzles are **increased by 25%**. The core is modeled as a spatially uniform ^{235}U fission source. The elevation view is at **292.5**°, the location of the outlet nozzle. The fast flux ratio in the RV and the nozzle is shown using flooded contours and contour lines. All other regions are colored based on their material assignments. The values inside the shaded boxes are the minimum and maximum ratios in the RV and the nozzle at this azimuthal angle. The minimum and maximum values in (b) are shown separately for the portions of the RV below and above 402.59 cm, where the thickness of the RV changes.

9 Effect of Thermal Insulation between the Reactor Vessel and the Bioshield

Reactor pressure vessels for PWR and BWR designs have a layer of thermal insulation between the vessel outer radius and the inner radius of the concrete bioshield. This insulation layer has a minor effect on fast flux levels in the RV in the beltline region, where it can cause very slight increases in the fast flux levels at the outer surface of the RV due to backscatter of neutrons from the insulation. At locations outside the beltline region the presence of the insulation can reduce fast flux levels in the RV due to neutron attenuation in the cavity gap streaming region.

To assess the effect of thermal insulation, the PWR reference model was modified to include a thermal insulation layer modeled with a thickness of 8 cm using the material definition for PWR thermal insulation in NUREG/CR-6115 [19]. This insulation thickness was selected based on the cavity gap width in the reference PWR model. The axial extent of the modeled insulation is from near the bottom of the lower cylindrical portion of the RV to the elevation of the nozzle tunnels. Note that changes in the thickness, axial extent, and/or the insulation composition would affect the neutron transport behavior in the cavity region.

The effect of this insulation modeling is illustrated at two azimuthal locations in Figures 102 and 103. While there is no significant effect within the beltline region, the reduction in cavity streaming leads to a reduction of up to ~15% in the fast flux in the RV at locations where cavity streaming dominates the fast flux profile in the RV.

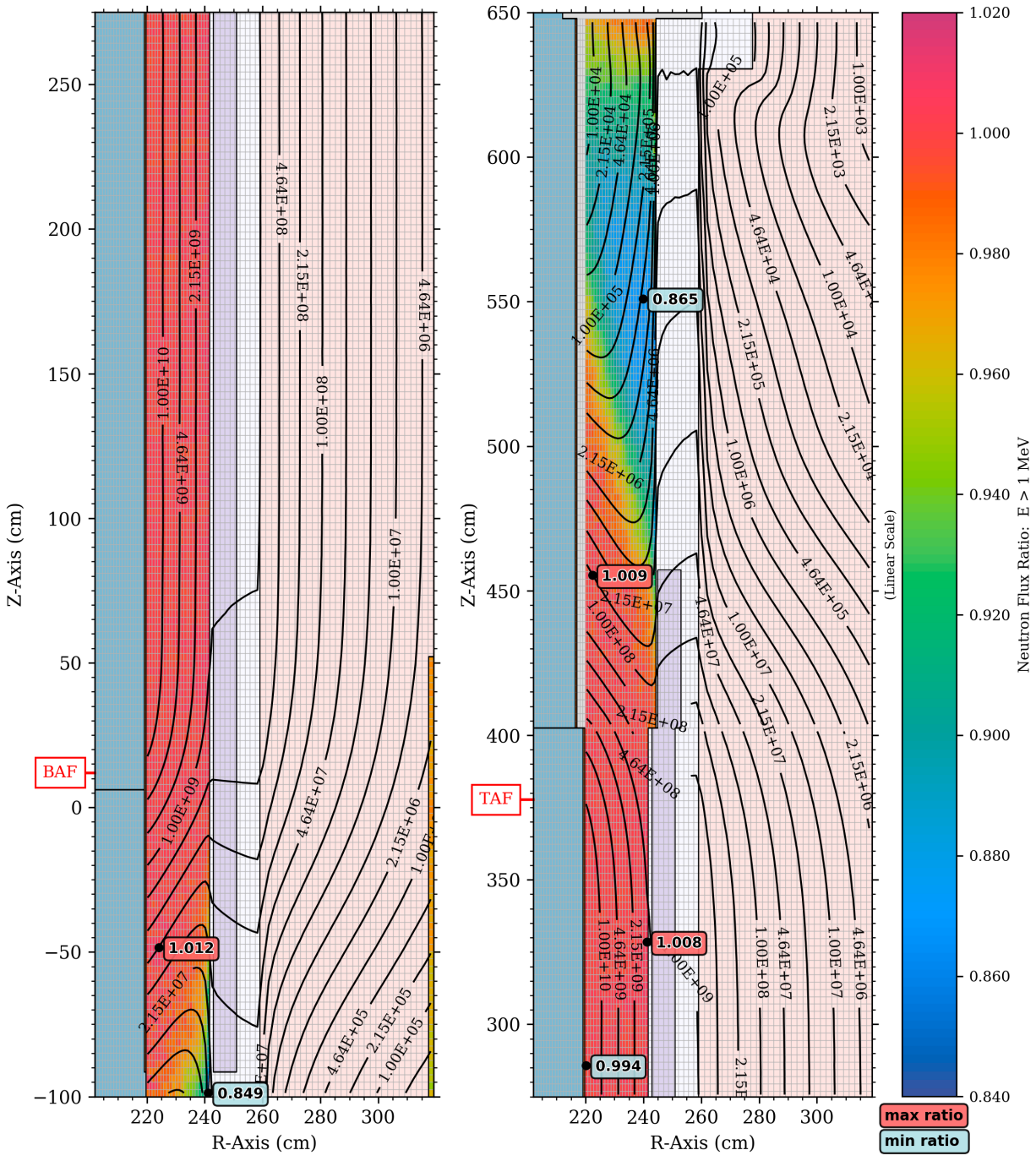

(a) Z = -100 to 275 cm

(b) Z = 275 to 650 cm

Figure 102. Fast neutron flux (E > 1 MeV) in the PWR reference model, and the fast flux ratio for a model that includes thermal insulation between the RV and the bioshield. The core is modeled as a spatially uniform ^{235}U fission source. The elevation view is at **270.5**°. The fast flux ratio in the RV, which has the maximum amount of water between the core and the RV is shown using flooded contours. All other regions are colored based on their material assignments. The flux levels for the reference model are shown using contour lines. The values inside the shaded boxes are the minimum and maximum ratios in the RV, which has the maximum amount of water between the core and the RV at this azimuthal angle. The minimum and maximum values in (b) are shown separately for the portions of the RV below and above 402.59 cm, where the thickness of the RV changes.

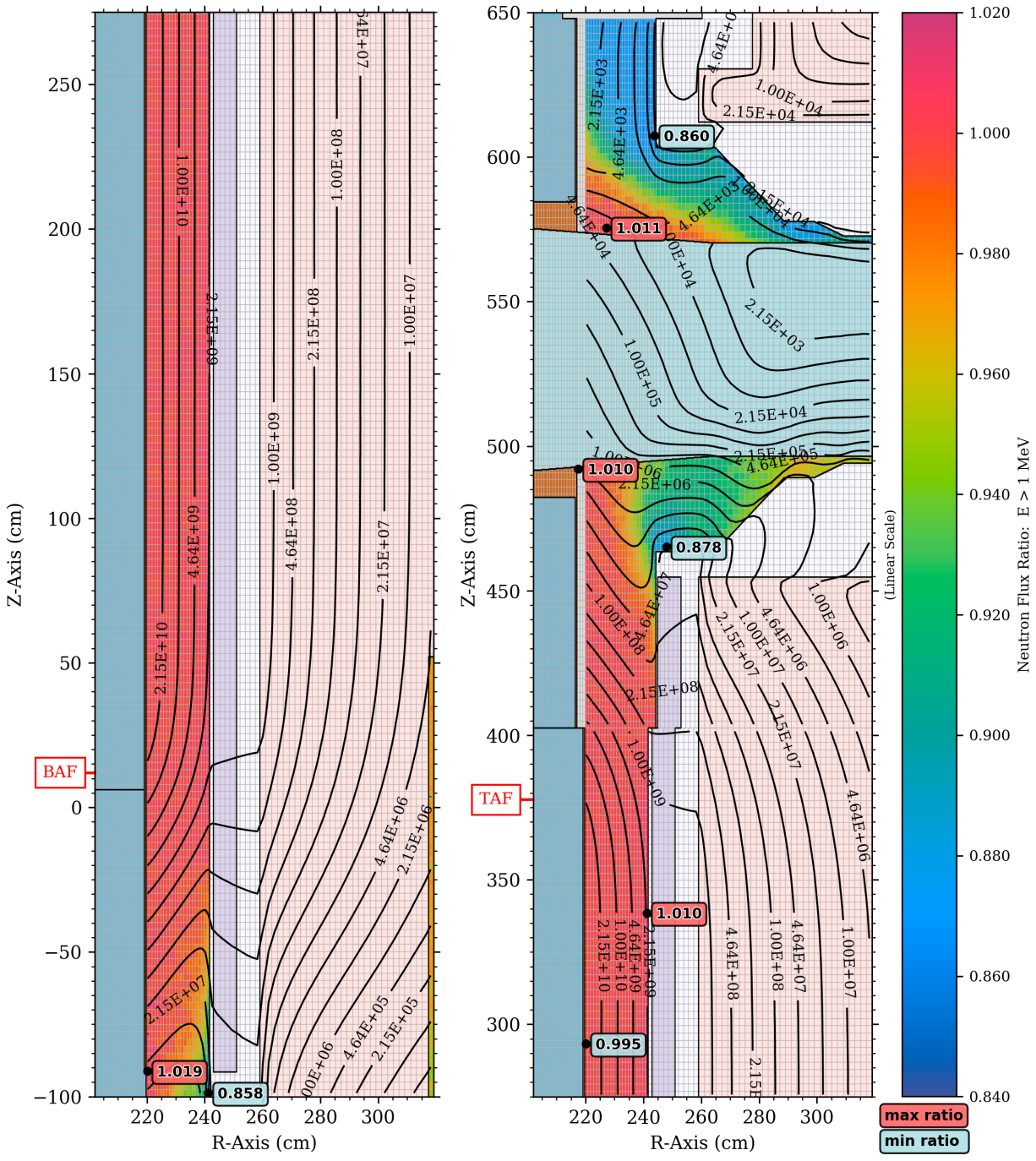

(a) Z = -100 to 275 cm

(b) Z = 275 to 650 cm

Figure 103. Fast neutron flux (E > 1 MeV) in the PWR reference model, and the fast flux ratio for a model that includes thermal insulation between the RV and the bioshield. The core is modeled as a spatially uniform ^{235}U fission source. The elevation view is at **292.5**°. The fast flux ratio in the RV, which is the centerline of the outlet nozzle is shown using flooded contours. All other regions are colored based on their material assignments. The flux levels for the reference model are shown using contour lines. The values inside the shaded boxes are the minimum and maximum ratios in the RV, which is the centerline of the outlet nozzle at this azimuthal angle. The minimum and maximum values in (b) are shown separately for the portions of the RV below and above 402.59 cm, where the thickness of the RV changes.